Design of an Eddy Current Probe for Cancer Detection

Undergraduate Thesis

Presented in Partial Fulfillment of the Requirements for Undergraduate Research in the College of Engineering of The Ohio State University

By

Scott Koch

Department of Mechanical and Aerospace Engineering

The Ohio State University

2014

Defense Committee:

Prof. Vish Subramaniam, Advisor

Prof. Shaurya Prakash

_____

Approved: Prof. Vish Subramaniam

Abstract

Surgery is the main treatment option for solid tumors. Surgeons use palpation and sight to identify and remove these malignant tumors during surgery. Surgically excised tissue are marked only at a few locations for pathological analysis so that much less than 1% of the excised tissue is actually analyzed. Analysis of all removed tissue could enable surgeons to decide in real-time whether or not more surgical intervention is necessary. The overall goals of this research are (1) to develop a tool that surgeons can use to quantify the boundaries of tumors embedded in excised tissue, and (2) to provide an objective basis for determining in real-time whether or not any additional surgical intervention is necessary while the patient is still in the operating room (OR). Recent work at OSU has shown that eddy currents induced in tissue by a time-varying magnetic field can be used to distinguish between cancer-bearing and normal tissue. The objectives of this project are to design, construct, and optimize an eddy current detector for real-time detection of malignant solid tumor boundaries. The eddy current probe comprises two coaxial coils, the inner of which is the primary and the outer serves as the detector. Inter-layer effects are explored by removing a detector coil layer from a previous probe design and the effect of the probe's intrinsic capacitance is explored by varying the insulation

thickness of the probe wires. The probes are then characterized and evaluated using measurements on animal tissue. It is found that removing a layer of windings in the detector coil sharply reduces the detector coil's inductance and voltage signal when measuring tissue. Furthermore it is found that the intrinsic probe capacitance due to wire insulation thickness also affects the detector signal, but to a lesser extent than removing a detector coil layer. Both the number of detector coil layers and intrinsic probe capacitance affect the ability of the eddy current probe to detect tissue and determine contrast between tissue types.

Dedication

Dedicated to my family and friends

Acknowledgements

I would like to thank my advisor, Vish Subramaniam, for his extensive support and guidance. I have learned so much from him over the course of this research.

I would like to thank Joe West for his ingenuity and assistance.

I would like to thank Emily Sequin, Travis Jones, Brad Smith, and Anu Kaushik for the enjoyable time spent in the lab.

Finally, I would like to thank my parents, Rick and Lisa, and siblings, Lori and Andy, for their love and support.

Vita

February 7, 1992	……	Born – Cincinnati, OH, USA
2010 to 2014	……	Mechanical Engineering Undergraduate, Department of Mechanical and Aerospace Engineering, The Ohio State University

Fields of Study

Major Field: Mechanical Engineering

Table of Contents

List of Figures

List of Tables

List of Equations

Chapter 1: Introduction

1.1 Motivation for Cancer Detection

Cancer is the uncontrollable division of cells, forming tumors which spread throughout the body via the blood or the lymphatic system. The National Institutes of Health estimates that in 2013 alone, there were 1,590,550 new cases and 561,330 deaths due to cancer involving solid tumors [1]. There is therefore a considerable ongoing effort to better the detection and removal of cancer [2, 3, 4, 5].

A majority (>50%) of solid malignant tumors are treated by surgery [6]. A successful surgery, however, requires the removal of all cancerous tissue from the patient. This necessitates the ability to discern between tumor and normal tissue. Advanced diagnostics before and after surgery, such as CT scans, PET scans, and MRI, are the best detection methods currently available. However, there is presently no tool for detecting cancer during surgery, and surgeons must rely on merely sight, touch, and experience. When surgeons instruct pathologists on where to direct their examination for diagnoses, the same subjective manner is employed.

The goal of this research is to develop a tool that surgeons can use to quantify the boundaries of tumors embedded in excised tissue and to provide them with an objective basis for determining whether or not more tissue needs to be removed while the patient is still in the operating room.

1.2 Current Cancer Detection Methods

There are several pre-operative and post-operative cancer detection methods already in existence. This section reviews these methods and how their application to intraoperative or perioperative detection is limited.

Computed tomography, or more simply CT, is an imaging technique involving the use of x-rays passed through the body. Diverse parts of the body attenuate the wavelengths of the x-rays differently according to their densities and detectors are able to construct two-dimensional images of layers within the body [7]. CT is limited to a spatial resolution of a few millimeters at best and is non-specific so that the possibility of false positives is high. Moreover, its use in the operating room (OR) is further limited because of bulk and cost.

Positron emission tomography, better known as PET, involves introducing radionuclide tagged tracer molecules (FDG or deoxyglucose tagged with ^{18}F) into the patient that travel and collect in areas of the body with higher metabolic rates [7]. Detectors are then able to detect the gamma rays emitted from the decay of the tracers. This technique depends on cancer cells having higher metabolic rates and therefore false positives are possible in cells with high metabolic behavior such as in cases of inflammation. Furthermore, the radioactive molecules used in PET scans can be harmful to the caregivers (surgeons and nurses) in prolonged use.

Magnetic resonance imaging, also known as MRI, implements the use of magnetic fields to detect different structures within the body. Although this method produces high resolution images, it requires a motionless sample which is difficult in an abdominal surgical setting where motion is inevitable due to the patient's breathing.

The aforementioned techniques are in addition bulky, costly, and cumbersome rendering their utility in intraoperative and perioperative use to be limited.

Chapter 2: Background

2.1 New Cancer Detection Method

Recent work at Ohio State has taken advantage of the electrical properties of tissue in order to detect cancer [8, 9, 10]. Time-varying magnetic fields inducing eddy currents can be used to distinguish between normal tissues and cancer because of their differences in electrical conductivity and morphological structure. These eddy currents flow with different magnitudes and directions based on the conductivity and structure of the medium in which they are induced. A non-contact electromagnetic probe inducing and measuring eddy currents in tissue can therefore be of potential use in detecting cancerous tissue.

2.2 Non-Contact Eddy Current (EC) Probe Design

A dual coil eddy current (EC) probe is presently being used at OSU to induce and measure eddy currents in tissue. As shown schematically in Figure 1, the inner coil is the primary side and the outer coil is the detector side.

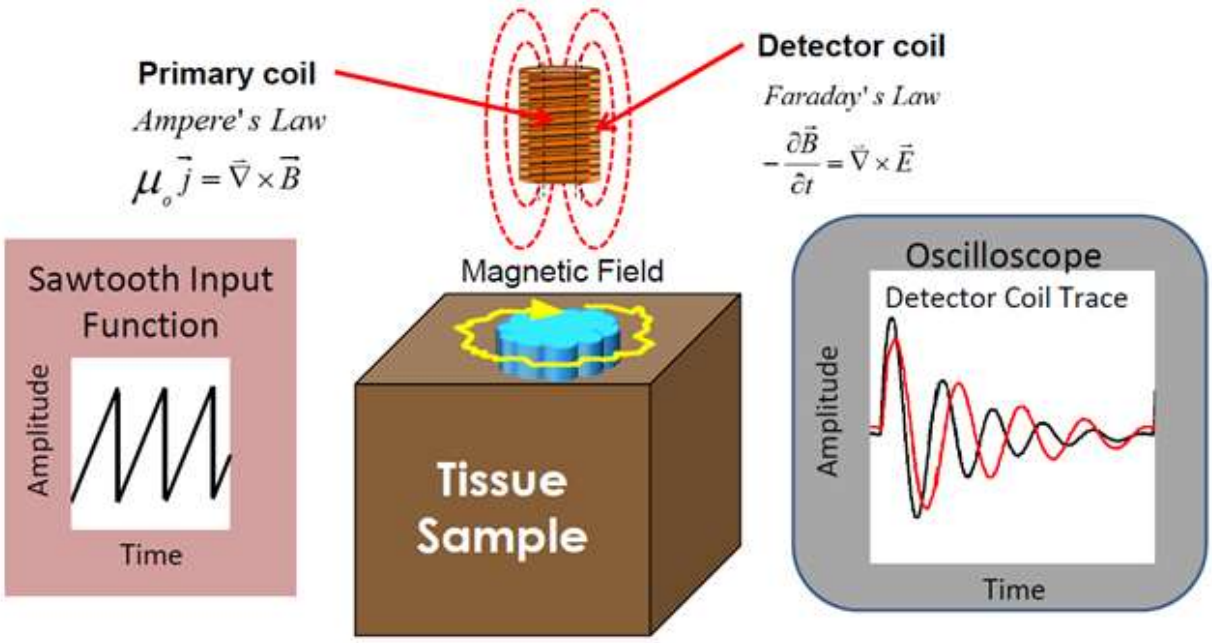

Figure 1: Dual Coil Probe and Tissue Sample

When a time-varying voltage, e.g. the sawtooth function in Figure 1, is applied to the primary coil, a magnetic field is generated by Ampere's Law. This magnetic field, shown by the dashed red lines in Figure 1, produces an electric field by Faraday's Law which in turn produces a magnetic field that induces a current and corresponding voltage in the detector coil. When brought near a sample, as shown in Figure 1, the magnetic field around the EC probe is affected by induced eddy currents and is recorded as a change in the signal observed in the detector coil.

Previous work has found that a sawtooth input to the primary coil generates a decaying sinusoidal voltage signal in the detector coil. With the introduction of a conducting sample, such as tissue, this detector signal changes in both magnitude and phase (i.e. shifts in time). The detector voltage shown by the black curve in Figure 1 represents when no sample is present and the detector voltage shown by the red curve in the figure represents when a sample is present. Changes in both the amplitude of the

peaks and the time between peaks and are detected using lock-in amplification. Furthermore, the type of tissue brought near the probe affects the magnitude and phase differently, so that lock-in amplification is able to differentiate between dissimilar types of tissues.

2.3 Previous EC Probe Design

A previously described dual coil design, referred to as B1, has been successfully used to detect the difference between normal and cancerous tissue [8]. B1 is wound with 32 gauge wire and has 2 layers on the primary coil side, 5 layers on the detector coil side, a length of 0.66 in, an inner diameter of 0.216 in, and an outer diameter of 0.326 in [8]. Figure 2 shows B1 as well as a surgically excised liver metastasis specimen that has been measured in three different locations with varying distance from the tumor (which is at location 3) [Emily Sequin, personal communication, March 20, 2014].

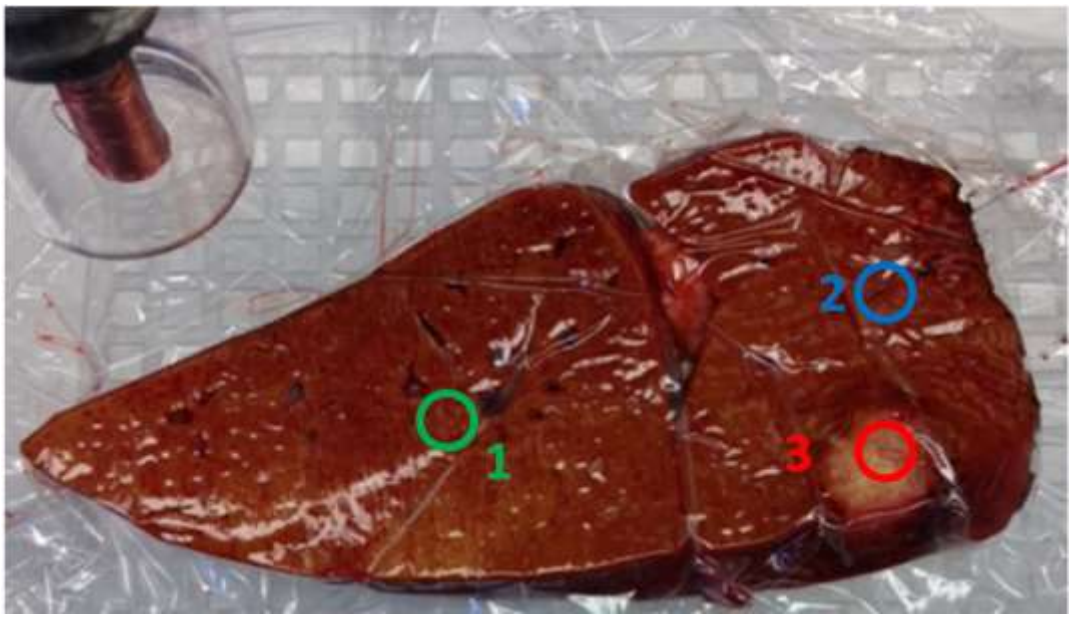

Figure 2: Cancer Detection of an Excised Liver Metastasis

The lock-in amplifier outputs a single voltage, V_{DC}, that accounts for both magnitude and phase changes. In Figure 3, the difference between this voltage at a null position away from tissue and at the location being measured on the tissue is plotted for each of the three points labeled in Figure 2. It can be seen that as the tumor is approached, the voltage difference decreases.

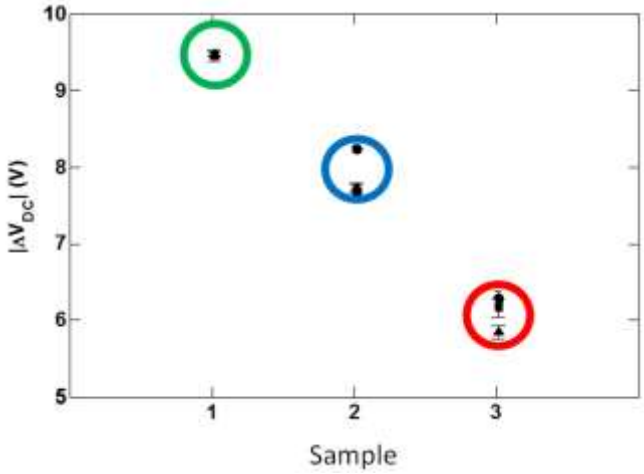

Figure 3: Voltage Difference for Three Locations Approaching Tumor

Figure 2 and Figure 3 show the successful detection of cancerous tissue using an EC probe. This EC probe design can however be improved. The odd number of layers in B1's detector coil is not desired because the two ends of the wire used to wind the coil are on opposite ends of the probe. This requires the wire at the bottom of the probe being brought back to the top so the circuit can be connected. The manner in which this wire is returned to the top of the probe can affect the magnetic field and overall sensitivity of the probe itself and can introduce spurious azimuthal orientation dependence. Furthermore, intrinsic capacitive effects within the EC probe are not fully understood. Therefore, the development of a new EC probe design is desired to explore these two areas.

Chapter 3: Experimental Methods

3.1 Development of the C-Series of Probes

In order to investigate the effects of the number of detector layers and intrinsic capacitance within the EC probe design, a new series of probes is developed and titled the C-Series. These EC probes, labeled C1 through C4, are shown in Figure 4.

Figure 4: C-Series of EC Probes

The C-series of probes are similar to the B-series except for two main, systematic differences. First, one detector layer is removed to allow for an even number of layers

and for the wire leads to be on the same end of the probe. B1 has 5 detector layers while the C-Series has 4 detector layers. Furthermore, wire insulation thickness is varied in the C-series to explore the effects of intra-coil capacitance. C1 and C4 are wound with 32 gauge wire (McMaster, 7588K88) with a radial insulation thickness of 0.001 in, while C2 and C3 are wound with 32 gauge wire obtained from Magnet Wire Supply (MWS, 32 SPN-155 RED NEMA MW80-C) with a radial insulation thickness of 0.0004 in.

The C-Series of EC probes are wound around a nylon core for two reasons. One, a non-conducting central core is required for the probe because it operates with the use of a magnetic field and any conducting material would alter this field. Two, a supporting structure connected to the core allows the probe to be connected to fixtures such as motorized stages for measurements. Figure 5 shows a 3/8 in diameter nylon rod with 0.7 in of one end lathed down to an average 0.215 in diameter. This is an average diameter because bending in the rod is unavoidable during the lathing process when the cutting tool touches the cantilevered nylon rod. Because of this bending, there is variance in diameter across the tip from a minimum diameter of 0.213 in to a maximum diameter of 0.218 in.

Figure 5: Nylon Rod with Lathed Tip

This nylon core is used for the winding of probe C1. Three more nylon rods are machined using a lathe to nominal diameters of 0.223 in, 0.211 in, and 0.215 in for C2,

C3, and C4 respectively with a tolerance of ±0.0001 in for all measurements. Each of these machined cores also has a varying diameter across its profile due to bending of the rod during the machining process, but the differences between maximum and minimum diameter for each core (0.024in, 0.019in, and 0.012in respectively) are considered small.

Coils are wound using a clamp to hold the nylon rod while the 32 gauge wire is hand-wound around the lathed tip. Figure 6 shows this process with the first layer of the primary coil being wound around the nylon core. The start of each coil is at the right next to the 3/8in end. Wrapping consistently and tightly packed to the left as far as possible completes the first layer of the primary coil. Continuing wrapping the wire consistently and tightly packing over this first layer and returning to the right, back to the start, completes the second and final layer of the primary coil.

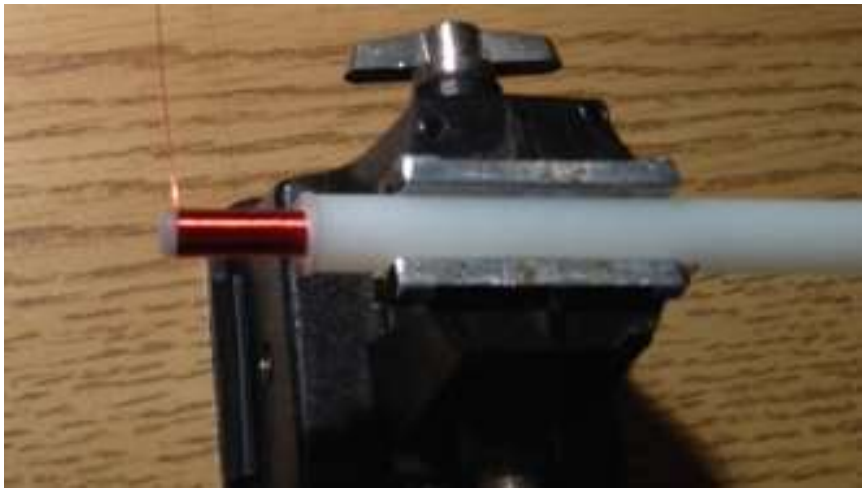

Figure 6: Wire Winding Process

After the two primary layers are completed, a layer of Clear Gloss 01 (Sally Hansen Hard as Nails Color) nail polish is applied to the outside of the primary coil to secure it when dried. The wire is then cut leaving enough extra length to connect to a

circuit board later. The detector coil is then wound around the primary coil using the same procedure except with four layers. Starting at the right again, the detector coil's first layer is wound to the left, the second layer is wound to the right, the third layer is wound to the left, and the fourth layer is wound to the right. After completion of the four layers in the detector coil, a layer of the nail polish is applied and allowed to dry and then the wire is cut. The final probe consists of two primary coil layers on the inside and four detector coil layers on the outside, each with approximately 65 turns per layer. It should be noted that while winding the outer layers, the act of winding the wire parallel becomes increasingly difficult and some scatter winding is unavoidable.

The fabrication process is repeated for probes C2, C3, and C4. Probes C2 and C3 are wound as similarly as possible with MWS wire with the thinner insulation thickness, while C1 and C4 are wound as similarly as possible with McMaster wire with the thicker insulation thickness. The final inner and outer average diameters and lengths of each probe are given in Table 1.

Table 1: Physical Dimensions of C-Series EC Probes (±0.0001 in Measurement Tolerance)

	C1	**C2**	**C3**	**C4**
Inner Diameter (in)	0.215	0.223	0.211	0.215
Outer Diameter (in)	0.328	0.313	0.310	0.310
Length (in)	0.685	0.684	0.642	0.651

Upon fabrication of each of the probes, it was found that the direction of the winding on one of the probes (C2) was not consistent. As shown in Figure 7, a coil can be wound either up or down (using the right hand rule). The direction of winding affects the direction of current flow and hence the direction of the magnetic field. This inconsistency is noted, however, and the direction of winding in each of the coils of the C-Series is displayed in Table 2.

C1, C3, and C4 have both coils wound in the same direction, but C2 has the primary and detector coil wound in opposite directions. This difference in the probes is noted and implies a magnetic field direction change as well as a detector voltage sign change.

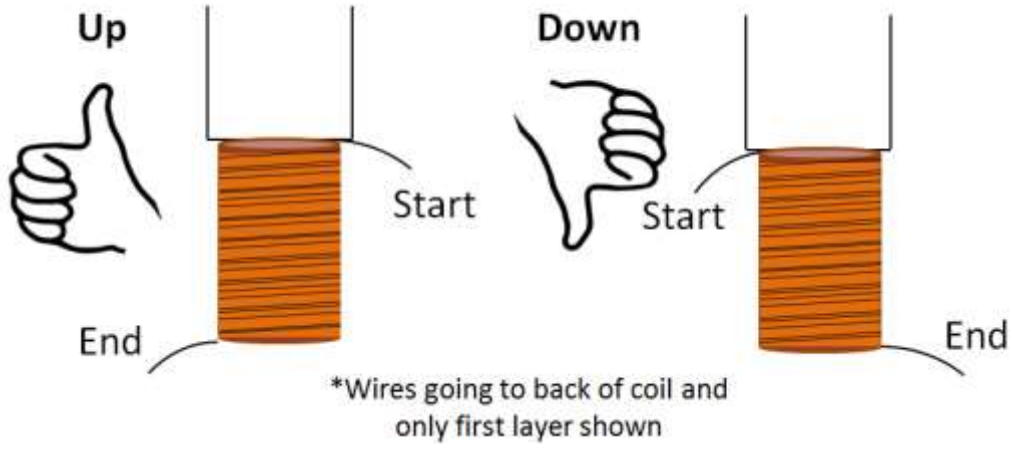

Figure 7: Wire Winding Direction

Table 2: C-Series Winding Direction

	C1	**C2**	**C3**	**C4**
Primary	Down	Down	Down	Up
Detector	Down	Up	Down	Up

The primary coil has an inner and an outer lead wire and the detector coil has an inner and an outer lead wire. The inner wire connects to the radially inward layer and the outer wire connects to the radially outward layer. The four total lead wires of the probe are covered with different colored shrink tubing and are soldered into a printed circuit board (PCB) as shown in Figure 8. Each of these wires has its own bus on the circuit board and a color code is used to differentiate between them. The inner wire of the primary is blue, the outer wire of the primary is white, the inner wire of the detector is purple, and the outer wire of the detector is green. The color of the shrink tubing used for each wire coordinates with this color code, but the shrink tubing is not heated because it holds more stiffness and support when it is unheated. In this manner, the shrink tubing serves as a color code as well as a protective layer around the wire. Four small wires with the same four colors are then soldered into their respective colored buses on the circuit board as shown on the right in Figure 8. These wires allow for the easy connection of micro-grabbers, which are also shown in Figure 8. Finally two 550 Ω ballast resistors are soldered into the PCB as shown in Figure 8. One resistor is soldered to the primary coil inner bus and the other is soldered to the primary coil outer bus. This allows for easy switching of the direction of the applied voltage in the primary coil without unsoldering and re-soldering, which can affect the overall capacitance in the circuit. The soldering of the PCB is repeated for all four C-Series probes.

In order to have a flat surface to contact tissue specimens, all four probes are then placed in 1mm thick glass housing and secured with electrical tape. These glass housings, shown in Figure 4, have large enough diameters that any envelopment of the tissue around them during an experiment would not affect the measurement.

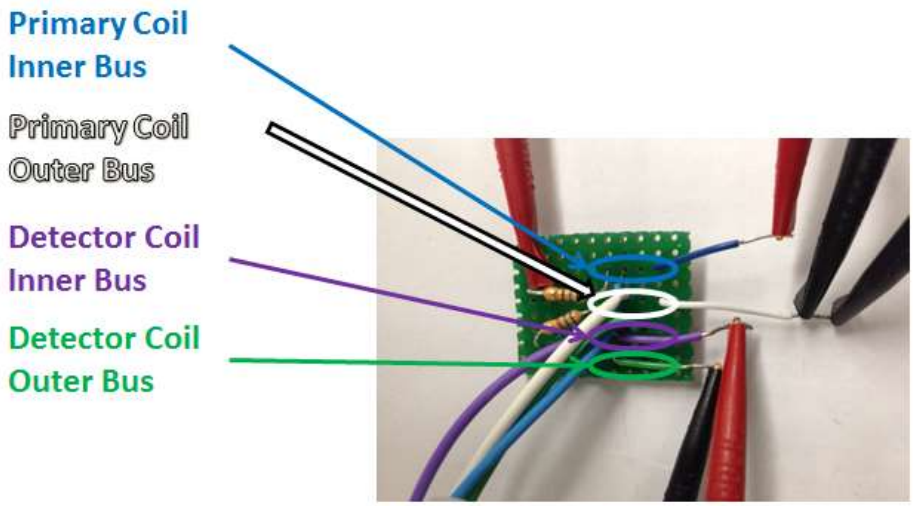

Figure 8: Printed Circuit Board

For all four probes, the resistances and self-inductances of the primary and detector coils are measured using an Extech Instruments LCR Meter (Model 380193) set at the 1 kHz setting. These measured resistances and inductances are given in Table 3.

Table 3: C-Series Resistances, Self-Inductances, and Mutual Inductances

	C1	**C2**	**C3**	**C4**
R_p (Ω)	1.68	1.77	1.78	1.62
L_p (μH)	26.4	31.5	30.2	22.7
R_d (Ω)	2.92	3.07	3.05	2.94
L_d (μH)	111.9	123.5	120.3	107.5
$M_{pd} = M_{dp}$ (μH)	46.9	56.4	56.5	44.6

The mutual inductances of each of the probes are then calculated using a MATLAB inductance calculator previously written for the dual coil probe design [10]. This calculator, given in Appendix A of this thesis, takes the probe length, wire diameter, inner and outer diameter of each coil, number of turns, and number of layers as inputs and calculates the self-inductances of the two coils and their mutual inductance as outputs. For each probe the calculated self-inductances are within 5 μH of the actual measured inductances. The measured self-inductances of the primary coils are 26.4, 31.5, 30.2, and 22.7 μH for C1, C2, C3, and C4 respectively. The measured self-inductances of the detector coils are 111.9, 123.5, 120.3, and 107.5 μH for C1, C2, C3, and C4 respectively. The uncertainty in these inductance measurements is 0.1 μH. The calculated mutual inductances for each of the C-Series probes are given in Table 3. The calculated mutual inductances of the probes are 46.9, 56.4, 56.5, and 44.6 μH for C1, C2, C3, and C4 respectively. It should be noted that mutual inductances M_{pd} and M_{dp} are taken to be equal.

The capacitances of the coils are difficult to measure because they are small. Previous studies have found that any capacitive buildup in the open circuit coil not currently being measured will result in an unrealistically high value of the measured capacitance [9]. The capacitances of the coils are therefore inferred by comparing with a model.

3.2 Inferring Capacitance

Capacitance is inferred through the use of a model. In order to understand the electrical properties of the EC probe and simulate the detector voltage signal, an electrical circuit element model is used as shown in Figure 9.

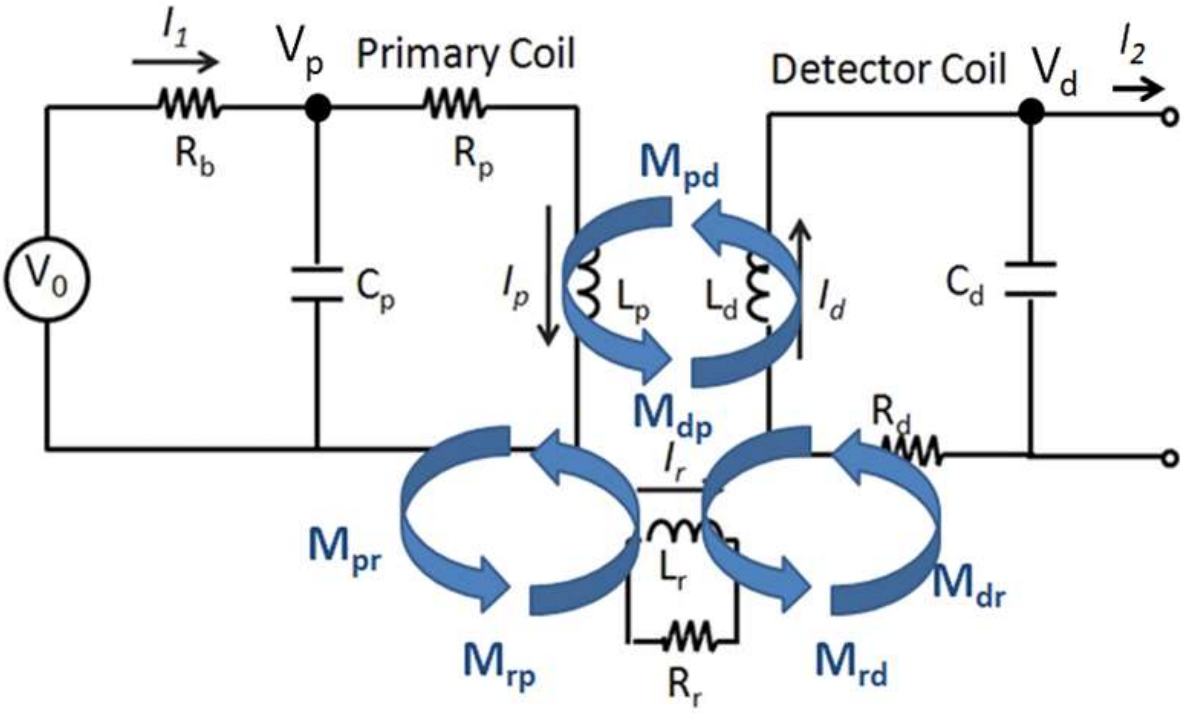

Figure 9: EC Probe Electrical Circuit Model

The left side of the circuit in Figure 9 represents the primary coil of the probe attached to the input voltage source through a ballast resistance. The primary coil is represented by a resistor and inductor in parallel with a capacitor. The resistor accounts for the conductivity of the wire, the inductor accounts for the rings of wire in the coil, and the capacitance accounts for the charge build-up between windings as well as between layers. The right side of the circuit represents the detector coil with the same electrical elements of a resistor and inductor in parallel with a capacitor. At the bottom of the diagram, an inductor and resistor represent the path of an eddy current in a sample. The primary coil, detector coil, and eddy current all interact with each other through mutual inductance. Because the primary and detector coils are inter-wound, they are mutually coupled and because the magnetic field of the EC probe is affected by the eddy current in the tissue, there is also mutual inductance between the tissue and the two coils.

When no sample is present, the bottom circuit elements become zero and the model simplifies to only the primary and detector coil circuits linked with a single mutual inductance assumed to be equal in both directions. Using this simplified electrical circuit model of the EC probe, the differential equations (Eq. 1, 2, 3 and 4) relating the primary coil to the detector coil can be written:

Equation 1: Primary Coil Current Law

$$\frac{V_o - V_p}{R_b} = C_p \frac{dV_p}{dt} + I_p$$

Equation 2: Detector Coil Current Law

$$C_d \frac{dV_d}{dt} = I_d$$

Equation 3: Primary Coil Voltage Law

$$V_p = R_p I_p + L_p \frac{dI_p}{dt} + M_{dp} \frac{dI_d}{dt}$$

Equation 4: Detector Coil Voltage Law

$$-V_d = R_d I_d + L_d \frac{dI_d}{dt} + M_{pd} \frac{dI_p}{dt}$$

These differential equations can be numerically solved for the voltages and currents in both the primary and detector coils. The simulated voltages of the primary and detector coils can then be compared with experimental voltages obtained. Because all parameters in the model besides the capacitances of each of the coils are measured or calculated, capacitance can be adjusted until the simulated and experimental results match.

Before actually inferring these capacitances, however, it is noted that because there are two coils with two lead wires, there are a total of four possible lead wire

arrangements with how the function generator and oscilloscope or lock-in amplifier can be connected to the probe.

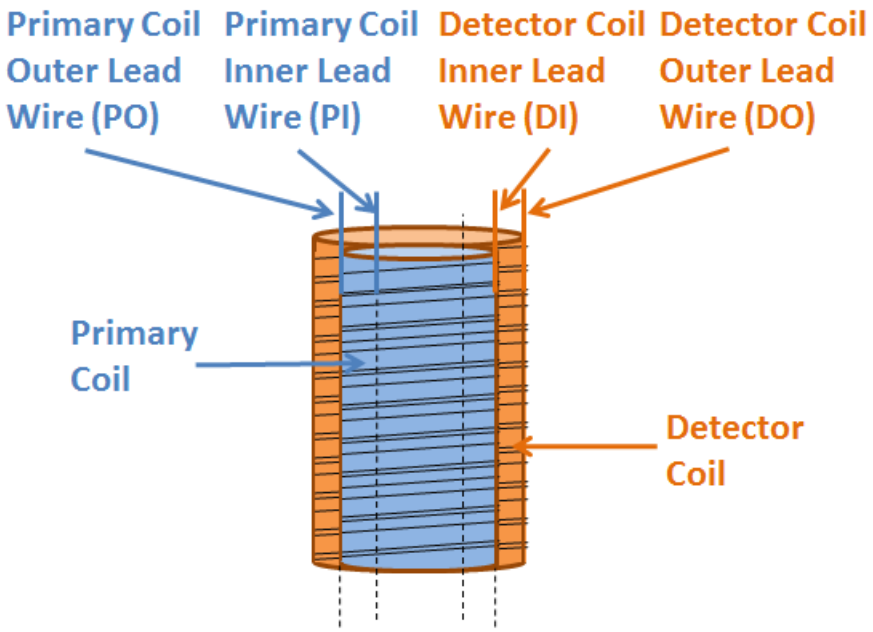

Figure 10: Four Lead Wires and Four Lead Wire Orientations

The positive lead of the function generator can connect with the primary inner (PI) or the primary outer (PO) wire. Also, the positive lead of the oscilloscope or lock-in amplifier can connect with the detector inner (DI) or the detector outer (DO) wire. There are therefore four total distinct lead wire orientations named based on where the positive lead of the signal generator and the positive lead of the oscilloscope or lock-in amplifier are connected. These four orientations are referred to here as PIDI, PIDO, PODI, and PODO. In this nomenclature, PIDI means that the function generator is connected to the primary coil's inner lead wire and the oscilloscope or lock-in amplifier is connected to the detector coil's inner lead wire.

Figure 11 shows the effect of changing orientations by monitoring the detector voltage signal for the four lead wire orientations of C1. When switching between these four lead wire orientations, not only is there a change in sign of the detector voltage signal, but there is also a change in magnitude and phase because the peaks of the ringing change in amplitude and shift in time. The PODI orientation in the top right quadrant of Figure 11 has less voltage amplitude in the first peak but much longer ringing than the PIDO orientation in the bottom left.

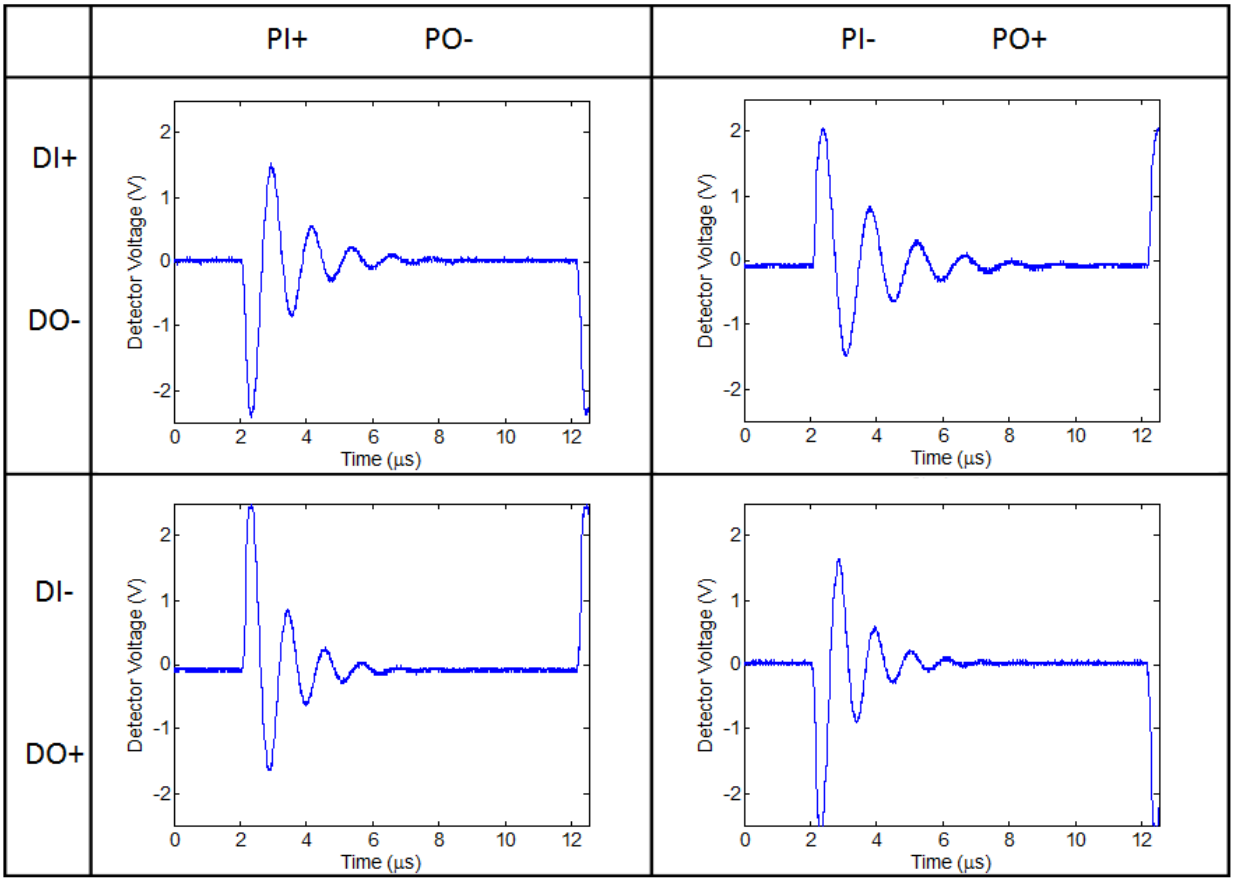

Figure 11: Detector Voltage Traces for C1 in All Orientations

It is important to be aware of how the probe is connected to the various instruments due to the fact that there are multiple layers in each coil and the skin depth of

the magnetic field generated by each layer is limited. If the inner layer of the primary coil is connected to the function generator (PI orientation), the magnetic field it creates will not affect the detector coil as strongly as if the function generator was connected to the primary coil's outer layer (PO orientation). This is because in the former case of PI, the magnetic field must permeate through the outer primary coil layer before interacting with the windings of the detector layers. Because of this skin depth effect, there is a decrease in magnitude of the magnetic field as it permeates through the extra coil layer.

In total, there are four possible orientations for a probe and capacitance can be inferred for each of them. This is accomplished by connecting each probe in each orientation, recording an experimental oscilloscope trace of the primary and detector voltage traces, and comparing the experimentally measured voltages to simulated voltages. These voltage traces are imported into MATLAB and compared (Appendix B). Figure 12 shows the graphical interface used to infer the capacitance with primary and detector voltage traces. All simulated inputs are known, measured, or calculated except for the capacitances. Experimental inputs allow the user to choose which probe and orientation to examine as well as whether the first peak in the detector voltage is positive or negative. When the capacitances in the model are systematically varied so as to match the experimental traces, the inferred capacitance of the probe is recorded.

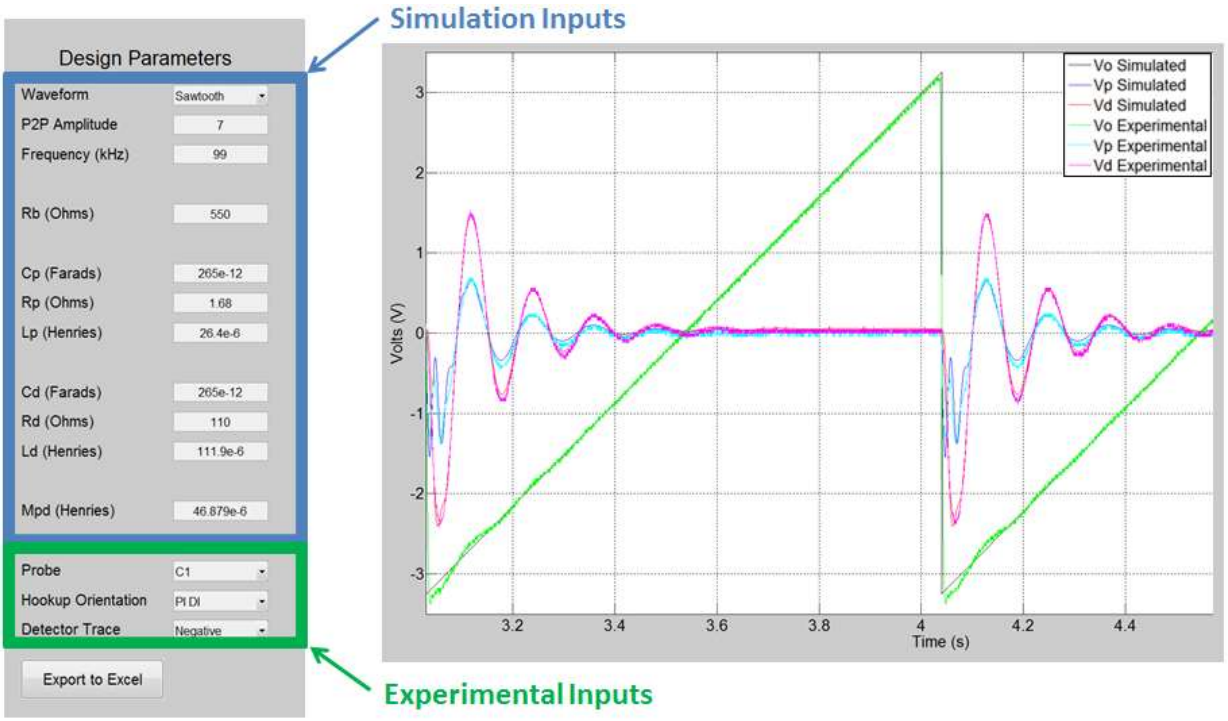

Figure 12: MATLAB Graphical Interface to Infer Capacitance

In this procedure, it is noted that the magnitude of the peaks obtained in the simulations are larger than the magnitude of the peaks recorded in the experiments. Adjusting capacitance allows for the phase of the peaks to align, but in order to align the magnitudes, detector resistance must be increased. Increasing this resistance decreases the magnitude of the voltage peaks without altering their phase. The justification for increasing the required resistance in the detector coil is that one needs to account for the inductive impedance of the detector coil at the frequencies of interest (99 kHz) to the measurement.

In the numerical model, the adjustment of capacitance is what is implemented in order to align the phase of the experimental and simulated voltages. It is noted that the best alignment of experimental and simulated voltage traces occur when primary and detector capacitances are equal. This is not what would be expected for two coils with different numbers of layers, but is an equivalent capacitance used to mimic the probe

characteristics. The inferred capacitances are thus recorded for each of the four probes connected in each of the four lead wire orientations.

3.3 Experimental Apparatus

In order to conduct measurements on animal tissue with the C-Series of EC probes, a system is setup to control the probe and collect the data. The experimental apparatus used in this system is shown in Figure 13. A Hewlett Packard 33120A 15 MHz function waveform generator is used to drive a 7 Vpp, 99 kHz, sawtooth waveform through a 550 Ω ballast resistor and into the primary coil. Connected as shown in Figure 13, a Stanford Research System SR510 Lock-in Amplifier is used to measure both the amplitude and phase of the detector signal relative to the reference signal from the function generator. This lock-in amplifier is useful for this application because it is capable of accurately measuring small signals by reducing noise [11]. The DC voltage output from the lock-in is then connected to an Agilent DSO-X 2014A, 100 MHz, Oscilloscope. Data from the oscilloscope is collected on a flash drive in CSV format and transferred to a computer where it is saved and analyzed.

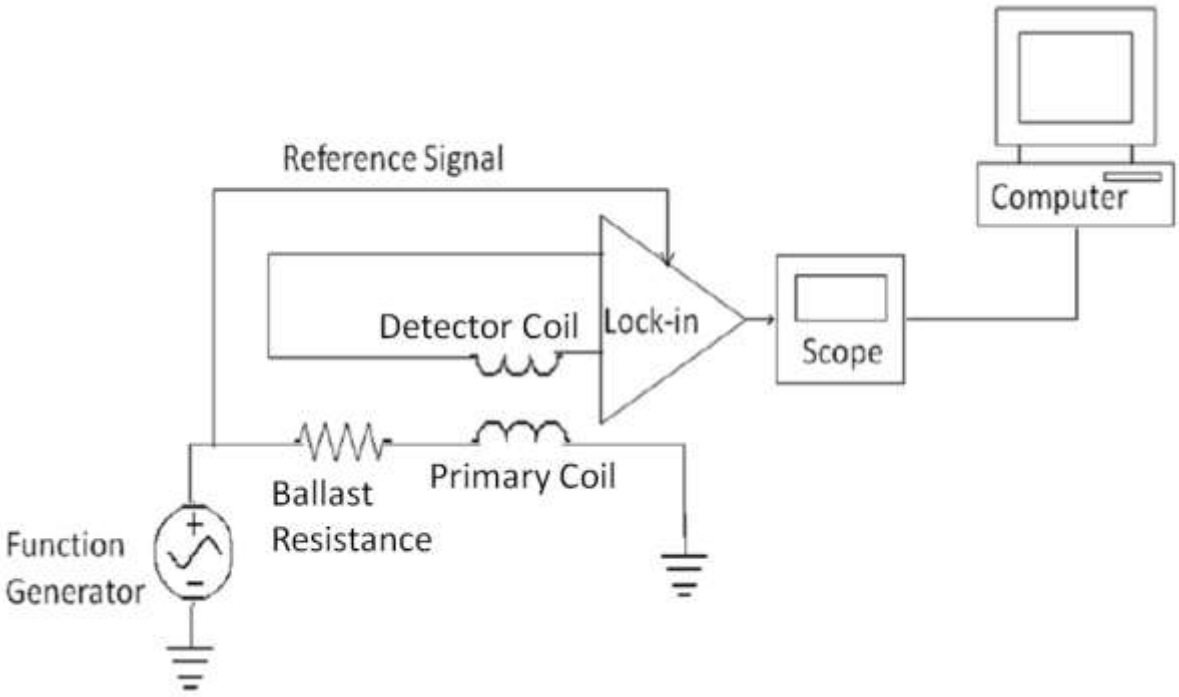

Figure 13: Experimental Apparatus for Data Acquisition

The SR510 Lock-In Amplifier is able to detect changes in both magnitude (V_i) and phase (Ø) according to Equation 5. The settings for the lock-in amplifier when it is used are given in Table 4.

Equation 5: Lock-In Amplifier Output Voltage

$$V_{DC} = 10A_e(A_V V_i cos\emptyset + V_{OS})$$

Where: A_e = 1 or 10 per the Expand setting

A_v = 1/Sensitivity

V_i = magnitude of signal

Ø = phase between signal and reference

V_{os} = offset (not used)

Table 4: Lock-In Amplifier Settings

Option	**Setting**
Input Signal	Detector Coil Voltage into Channel A
Reference Signal	7 Vpp, 99 kHz Sawtooth
Sensitivity	2mV
Dynamic Resolution	High
All Offsets	Off
Expand	X1
Mode	f
Trigger	~
Pre Time Constant	300ms
Post Time Constant	0.1s

3.4 Experimental Procedure

This section describes the procedures used to collect data in the experiments reported here. Measurements on animal tissue specimens of pork and beef are taken for all four probes in all four lead wire orientations described earlier. This allows the determination of the orientation that produces maximum signal between null and tissue as well as the orientation that offers maximum contrast between the two tissue specimens. After determining the optimum orientation, an external capacitor is soldered in parallel with the detector coil of each probe and measurements are repeated for the optimum orientation with the external capacitance added ranging from 10pF to 100pF in 10pF

increments. The added parallel capacitance in the external circuit has been recently found to optimize EC probe performance and overcome any drawbacks from the coil fabrication process [Travis Jones, personal communication, January 27, 2014].

Animal tissue samples are obtained from the Giant Eagle grocery store. Pork Loin Boneless Center Cut Chops and 80% Lean, 20% Fat Ground Chuck Beef are obtained and allowed to warm to room temperature over the course of approximately one hour. These two tissue samples are chosen because they have different morphological structures: pork being a relatively homogeneous tissue and ground beef being an extruded tissue packed together to have individual grains.

The pork tissue is then cut into two 1 in by 1 in by 0.5 in cubes and the ground beef is hand formed into two similar 1 in by 1 in by 0.5 in cubes in order to have samples of analogous volume. One pork cube is sealed in a storage bag and the two beef cubes are sealed in a separate storage bag in order to preserve their freshness while the first measurements are conducted on a pork sample without external capacitance. The other pork sample and one of the beef samples are used for measurements where external capacitance is added, while the other beef sample is measured without external capacitance as well.

A grounding wire is placed horizontally across a plexiglass stage and the first pork sample is placed on top of the wire in the center of the stage. Then plastic wrap is wrapped neatly around the tissue and secured down with electrical tape. The plastic wrap preserves the tissue over the course of the measurements and the tape prevents the plastic wrap from moving. The tissue setup on the plexiglass stage can be seen in Figure 14 for both pork and beef samples.

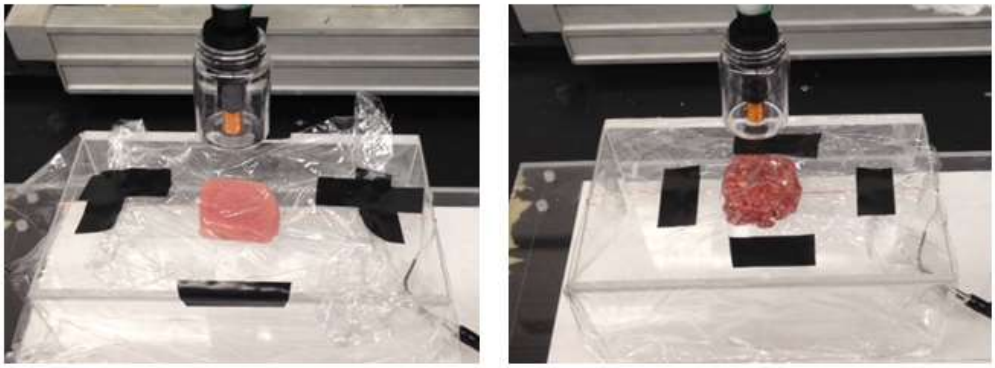

Figure 14: Pork and Beef Samples on the Plexiglass Stage

The 3/8 in diameter end of the first probe (C1), which has been connected to the apparatus discussed in the previous section, is then press fit into the wooden extension arm of the Velmex numerically controlled stage. The function generator, oscilloscope, and lock-in amplifier have been connected to the probe and running for an hour prior in order to achieve steady state operating conditions before any testing. This overall physical setup for animal tissue measurements is shown in Figure 15.

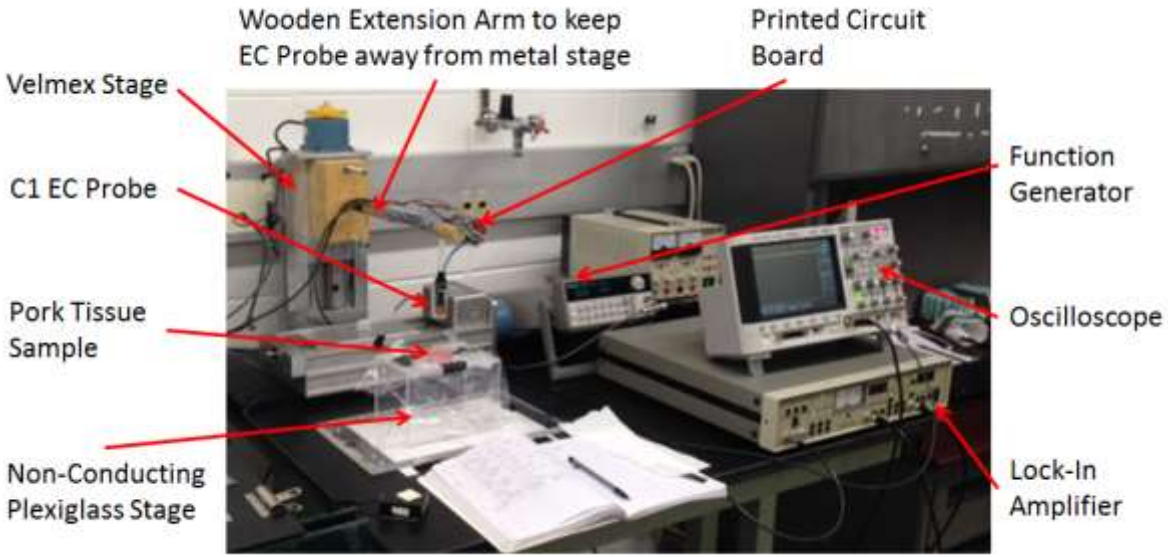

Figure 15: Physical Setup for Animal Tissue Measurements

Difficulties were encountered with fixturing using the Velmex stage. Consequently, the Velmex stage was not used and the plexiglass stage with the sample was manually raised up to the probe.

For the first probe (C1) and first orientation (PIDI), three repeated measurements of pork tissue are recorded. First, the reference phase of the lock-in amplifier is adjusted to produce an output voltage close to zero and the oscilloscope is set to start collecting data. Three seconds of data are collected, and then the stage and sample are raised to the bottom of the probe's glass housing where three more seconds of data are collected. This is repeated two more times for a total of three measurements with as constant a physical force applied as possible. The oscilloscope is stopped from recording any more data and the voltage trace from the lock-in amplifier is then saved. An example of the voltage detected by the lock-in amplifier for the three repeated measurements is shown in Figure 16. The peaks represent the null state away from the tissue and the valleys represent measurements taken on the tissue specimen.

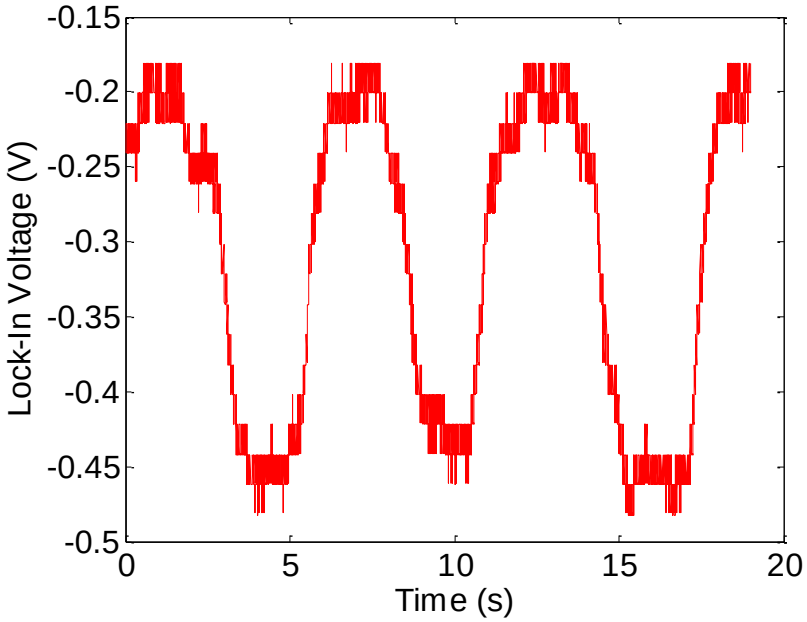

Figure 16: Three Repeated Measurements of Pork using C1 in the PODI Orientation

The differences between successive peaks and valleys are then calculated for a total of three measurements. The first, second, and third peaks are compared with the first, second, and third valleys respectively to represent the three different voltage changes obtained from the introduction of the tissue. This process of calculating voltage change is accomplished by averaging 500 data points, or 0.2s of data, at the peaks and valleys of the voltage data recorded by the lock-in amplifier. Data points are taken as far away as possible from the transient voltage change due to tissue movement. The first peak average voltage is then subtracted from the first valley average voltage to obtain the first change in lock-in voltage due to tissue. This is repeated for all three measurements for a total of three voltage changes. The average and 95% confidence interval of these three measurements is then calculated using Equation 6 and the student t-distribution. The t-distribution is used because the population standard deviation is unknown.

Equation 6: T-Distribution Confidence Interval

$$95\%\ CI = \bar{X} \pm t_{\propto,n-1} * \frac{s}{\sqrt{n}}$$

Where: $\bar{X}$ = average of samples

t = t-score associated with α and n

α = 1 – confidence level (1-95% = 0.05 in this case)

n = number of samples (3 in this case)

s = sample standard deviation

For the pork sample, this process of three repeated measurements and confidence interval calculation is followed for all four probes in all four orientations. The ground beef sample is then placed on the stage and the measurement process is continued again

for all four probes in all four orientations. With 4 EC probes, 4 lead wire orientations, and 2 tissue samples, a total of 96 measurements and 32 confidence intervals are calculated without external capacitance.

This data is then analyzed and the optimum orientation for each EC probe is determined. The optimum orientation is chosen based on the best voltage contrast between pork and beef specimens when at least a 0.1V signal is detected between null and tissue. A 0.1V threshold is determined based on ability to distinguish between null and tissue in the collected data because a difference in voltage of less than 0.1V is relatively difficult to discern.

For probe C1, external capacitance is then added by soldering a variable capacitor, shown in Figure 17, in parallel with the detector coil.

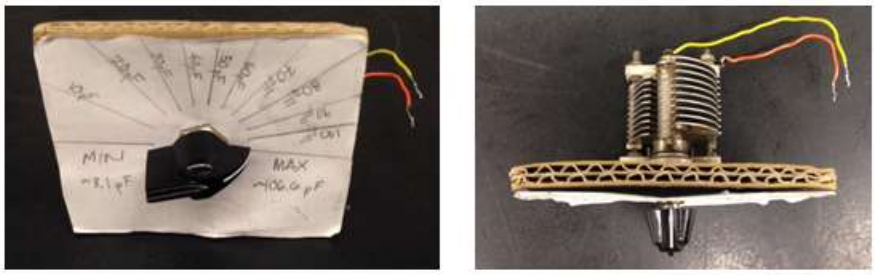

Figure 17: Variable Capacitor

Using the same procedure of three repeated measurements, measurements are taken on the remaining pork and beef specimens for external capacitance varying from 10pF to 100pF with 10pF increments. With 4 EC probes, 1 optimum lead wire orientation for each probe, 2 tissue samples, and 10 external capacitance increments, a total of 240 measurements and 80 confidence intervals are calculated with external capacitance.

Chapter 4: Results and Discussion

4.1 Comparison of B1 and C-Series EC Probes

The two systematic differences between B1 and the C-Series are number of detector layers and insulation thickness. B1 has 5 detector layers while the C-Series has 4 detector layers. Furthermore, C1 and C4 have a radial insulation thickness of 0.001 in while C2 and C3 have a radial insulation thickness of 0.0004 in. B1's insulation thickness is unknown but inferred to be 0.001 in by comparing the type of wire used with that available in the laboratory where B1 was developed. Including these two main differences between B1 and the C-Series, Table 5 compares the physical properties of all of these EC probes.

Table 5: Comparison of B1 and C-Series Physical Properties

	B1	Average of C-Series	C1	C2	C3	C4
Wire Gauge	32	32	32	32	32	32
Wire Insulation Thickness (in)	Unknown	N/A	0.001	0.0004	0.0004	0.001
Primary Layers	2	2	2	2	2	2
Primary Winding Direction	Unknown	N/A	Down	Down	Down	Up
Detector Layers	5	4	4	4	4	4
Detector Winding Direction	Unknown	N/A	Down	Up	Down	Up
Approximate Turns per Layer	75	65	65	65	65	65
Inner Diameter (in)	0.216	0.216	0.215	0.223	0.211	0.215
Outer Diameter (in)	0.326	0.315	0.328	0.313	0.310	0.310
Length (in)	0.66	0.665	0.685	0.684	0.642	0.651

As can be seen from Table 5, the similarities between B1 and the C-Series of EC probes include the wire gauge, number of primary layers, the inner diameter, and the length. Differences between B1 and the C-Series probes other than in the number of layers and insulation thickness are also apparent. The C-Series has approximately 10 less turns per layer compared to B1. The discrepancy in the number of turns per layer is due to both the imperfect hand-winding of the probes as well as the uncertainty in the counting of the number of turns. In any case, the less the number of turns, the smaller the inductance, which is also expected due to having one less detector layer. Another difference between B1 and the C-Series is the smaller outer diameter in the C-Series that can be explained by the C-Series having one less detector layer. Finally, the direction of wire winding also demarcates C2 as an outlier probe because it is the only one with its

primary and detector coils wound in opposite directions. These different winding directions would be expected to affect the magnetic field and detector signal, as is found and discussed in the next section.

The electrical characteristics of B1 and the C-Series coils can be compared as well. Table 6 shows the electrical properties of B1 and the C-Series. It should be noted that for the C-Series, the effective capacitances have maximum and minimum values since lead wire orientation affects intrinsic capacitance, as will be shown in the next section.

Table 6: Comparison of B1 and C-Series Electrical Properties

	B1	**Average of C-Series**	**C1**	**C2**	**C3**	**C4**
R_b (Ω)	830	550	550	550	550	550
R_p (Ω)	1.98	1.71	1.68	1.77	1.78	1.62
L_p (µH)	38.7	27.7	26.4	31.5	30.2	22.7
C_p (pF)	235	Min: 236 Max: 471	Min: 215 Max: 375	Min: 260 Max: 520	Min: 260 Max: 595	Min: 210 Max: 395
R_d (Ω)	5.59	3.00	2.92	3.07	3.05	2.94
L_d (µH)	330	115.8	111.9	123.5	120.3	107.5
C_d (pF)	235	Min: 236 Max: 471	Min: 215 Max: 375	Min: 260 Max: 520	Min: 260 Max: 595	Min: 210 Max: 395
M_{pd}=M_{dp} (µH)	94.1	51.1	46.9	56.4	56.5	44.6

The main similarities in electrical properties between the B1 and the C-Series are the primary resistance and inductance, which are expected because both probes have 2 layers in the primary coil. The slight decrease in the primary resistance and inductance of

the C-Series can be accounted for by approximately 10 less turns per layer. This as well as one less layer in the detector coil explains why the C-Series has less detector coil resistance and inductance. It is important to note that the removal of one detector layer drastically reduced the inductance of the detector coil by almost a third and the mutual inductance by half. B1 has a detector coil inductance on the order of 300 μH while the average detector coil inductance of the C-Series is on the order of 100 μH. Furthermore, B1 has a mutual inductance of approximately 100 μH while the C-Series has a mutual inductance of approximately 50 μH. It is also important to note that when comparing wire insulation thickness, C2 and C3 have thinner insulation thickness and higher inferred capacitance compared to C1 and C4. This is expected based on the equation for parallel plate capacitance, Equation 7. Even though this equation is not strictly valid for estimating the intrinsic capacitance within the coils, it can be used to infer that a thinner insulation would lead to decreasing the distance, L, between charged wires and increasing capacitance. The capacitances do not directly correlate however because the insulation thickness was decreased by a factor of 2.5 but the inferred capacitance only increased by approximately 20-40%. This discrepancy is due to the significant assumption made when comparing the EC probe to a parallel plate capacitor.

Equation 7: Parallel Plate Capacitance

$$C = \frac{\in A}{L}$$

Where: ∈=dielectric permittivity of the medium

A=Area of charged surface

L=Distance between areas

The final significant difference between B1 and the C-Series is the decrease in ballast resistance. The C-Series requires a lower ballast resistance of 550Ω compared to the 830Ω ballast resistance of B1 to obtain a similar magnitude in detector voltage signal. This is expected due to the smaller mutual inductance of the C-Series. Because the primary and detector coils in the C-Series of probes are less mutually coupled, the primary coil affects the detector coil less and a lower magnitude signal is obtained in the detector voltage. To counteract this, a smaller ballast resistance is used.

4.2 Capacitive Effects, Lead Wire Orientation, and Animal Tissue Measurements

Upon investigating the inferred capacitances for each probe in the C-Series, it is found that the inferred capacitance depends on the lead wire orientation of how the probe is connected to the function generator and the oscilloscope or lock-in amplifier. Figure 18 through 21 show the detector voltage traces for all four orientations of probes C1 through C4 respectively when they are away from tissue or any sample. As can be seen from these figures, changing the orientation of the probe affects more than just the sign of the detector voltage signal. Both the magnitude of the peaks and the time between peaks are affected when orientation is changed. Furthermore, because the phase or time between peaks changes, there is a noticeable change in inferred capacitance with a change in lead wire orientation. When lead wire orientation is changed, the percent difference between maximum and minimum inferred capacitance is 54%, 67%, 78%, and 61% for C1, C2, C3, and C4 respectively.

A common relationship between orientation and capacitance is found. For probes C1, C3, and C4, the PODI orientation is found to have the most elongated or maximum ringing while the PODO orientation is found to have minimum ringing. Additionally, in these three probes the PODI orientation has the largest inferred capacitance while the PODO orientation has the smallest inferred capacitance.

C2 does not follow this trend, however, because of the direction in which its coils are wound. Because the primary and detector coils of C2 are wound in opposite directions, the magnetic field it produces and the mutual coupling between the coils result in different detector voltage traces for each lead wire orientation. For C2, the maximum ringing and capacitance are found in the PIDI orientation while the minimum ringing and capacitance are found in the PIDO orientation.

When examining all C-Series probes as a whole, it is noted that as lead wire orientation changes, capacitance and therefore the amount of ringing and magnitude of peaks change. Moreover, certain orientations maximize or minimize capacitance and consequently ringing.

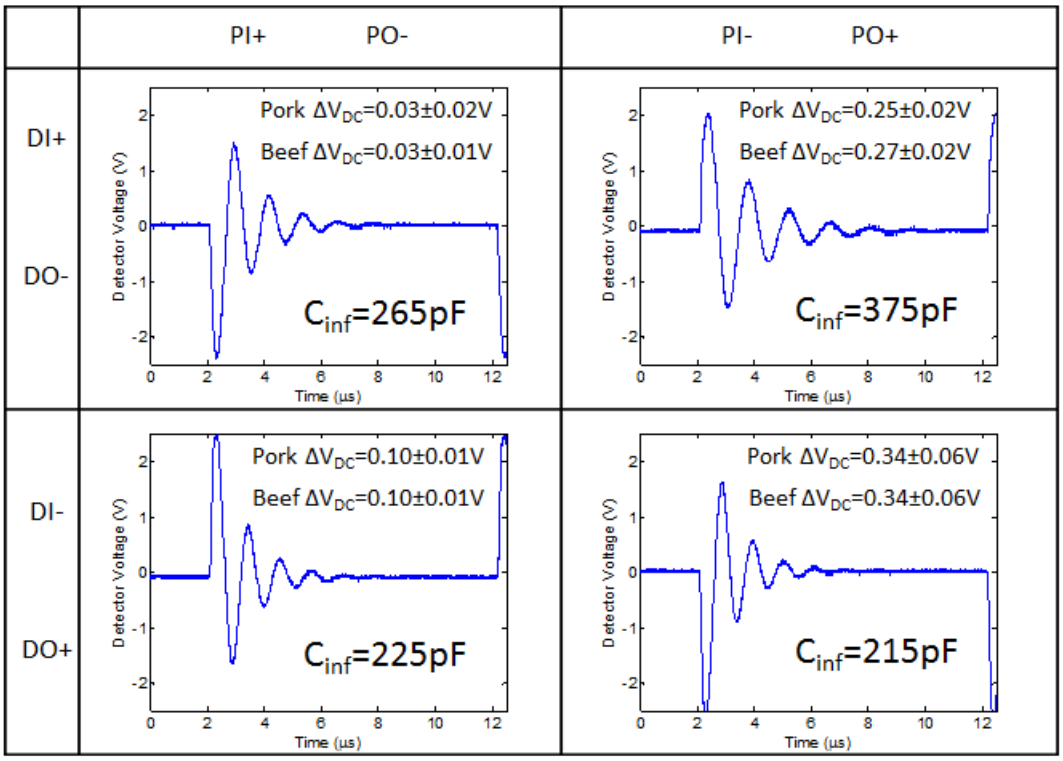

Figure 18: C1 - Detector Voltage, Inferred Capacitance, and 95% CIs for Tissues

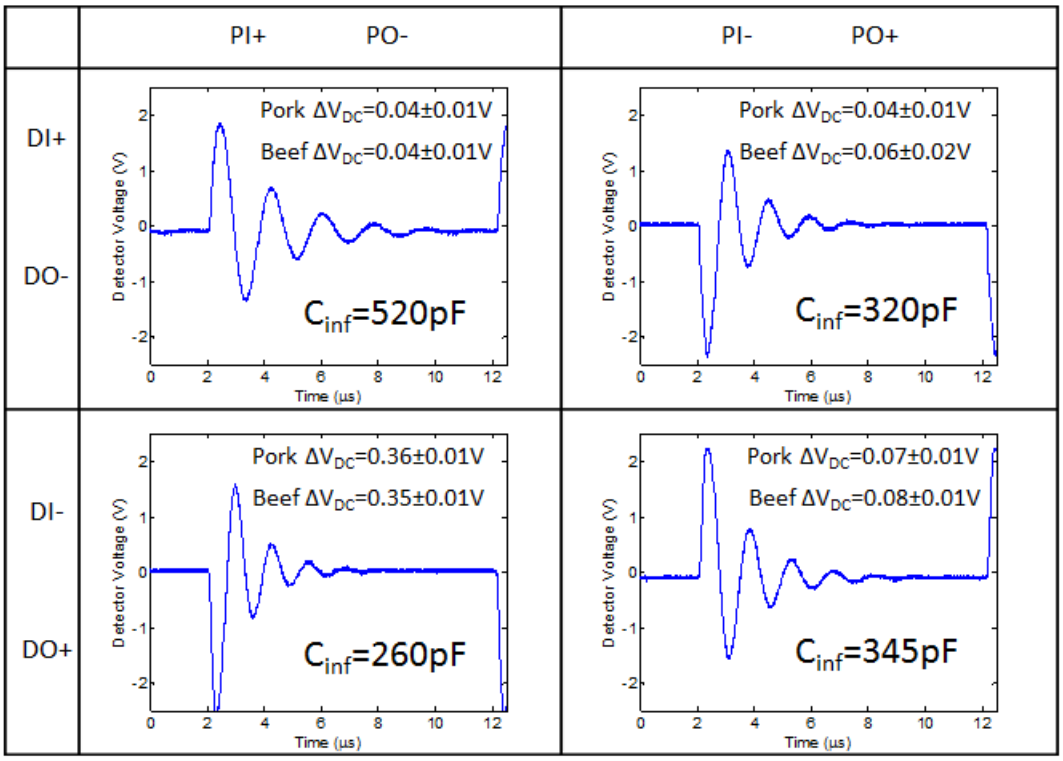

Figure 19: C2 - Detector Voltage, Inferred Capacitance, and 95% CIs for Tissues

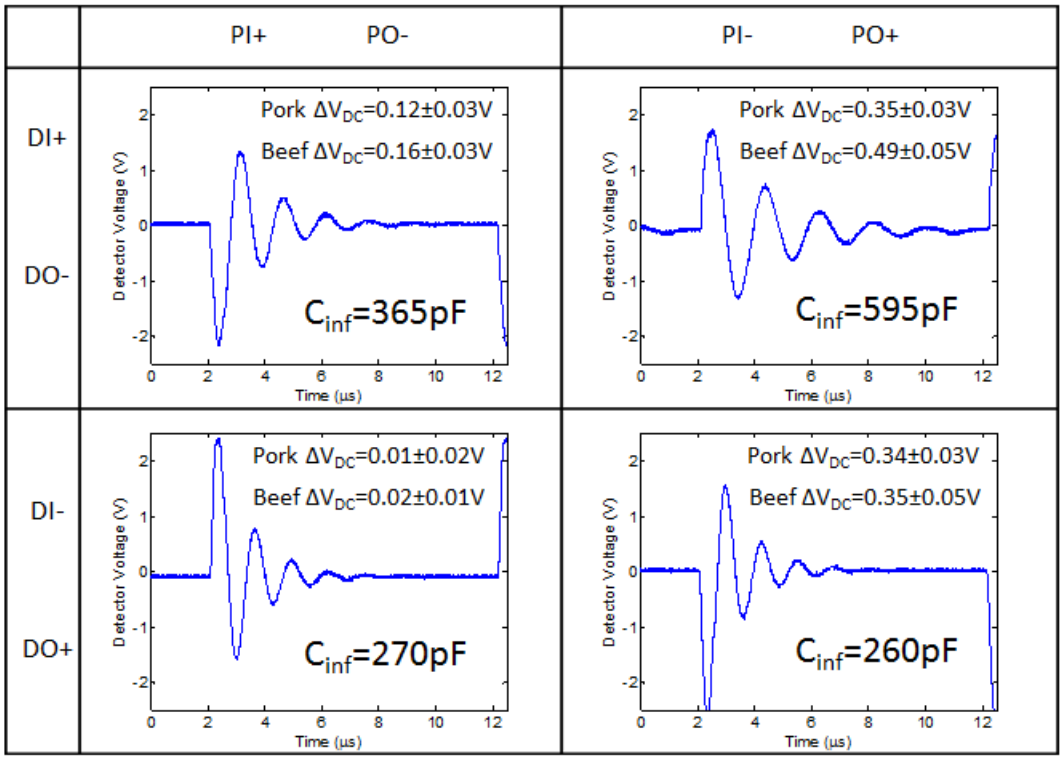

Figure 20: C3 - Detector Voltage, Inferred Capacitance, and 95% CIs for Tissues

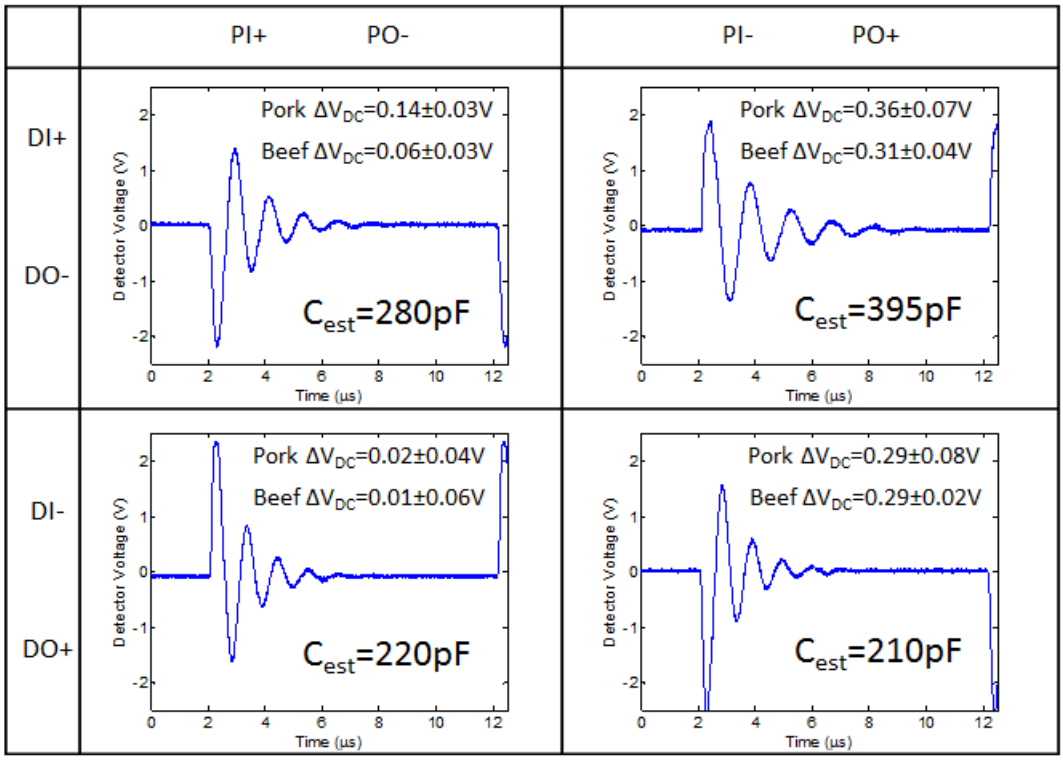

Figure 21: C4 - Detector Voltage, Inferred Capacitance, and 95% CIs for Tissues

Figure 18 through 21 also show the 95% confidence intervals for the animal tissue measurements conducted with all four probes in all four lead wire orientations. Again, a common relationship is evident when comparing the orientation of the connecting lead wires. For C1, C3, and C4, the PODI orientation results in maximum contrast between pork and beef while maintaining a voltage from the lock-in amplifier of at least 0.1V for both tissues. This PODI lead wire orientation, therefore, is found to be the optimum orientation for probes C1, C3, and C4.

C2, on the other hand, is the outlier probe with primary and detector coils wound in opposite directions. For this probe, the PIDO orientation is found to be the only orientation that is able to significantly detect a difference between no sample and a sample of tissue because only this orientation results in a change in voltage larger than

0.1V. This PIDO orientation is considered the optimum orientation for C2 even though only 0.01V of contrast between pork and beef is discernable.

4.3 External Capacitance

The effects of added external capacitance to the detector coil are investigated with each probe connected in its optimum orientation. These results are shown in Figure 22. For each probe, the addition of external capacitance affects the magnitude of voltage recorded by the lock-in amplifier as well as the contrast in voltage between specimens. The amount of change that this external capacitance produces, however, is relatively small and does not significantly improve the ability of any of the C-series probes to detect tissue or differentiate between different types of tissue.

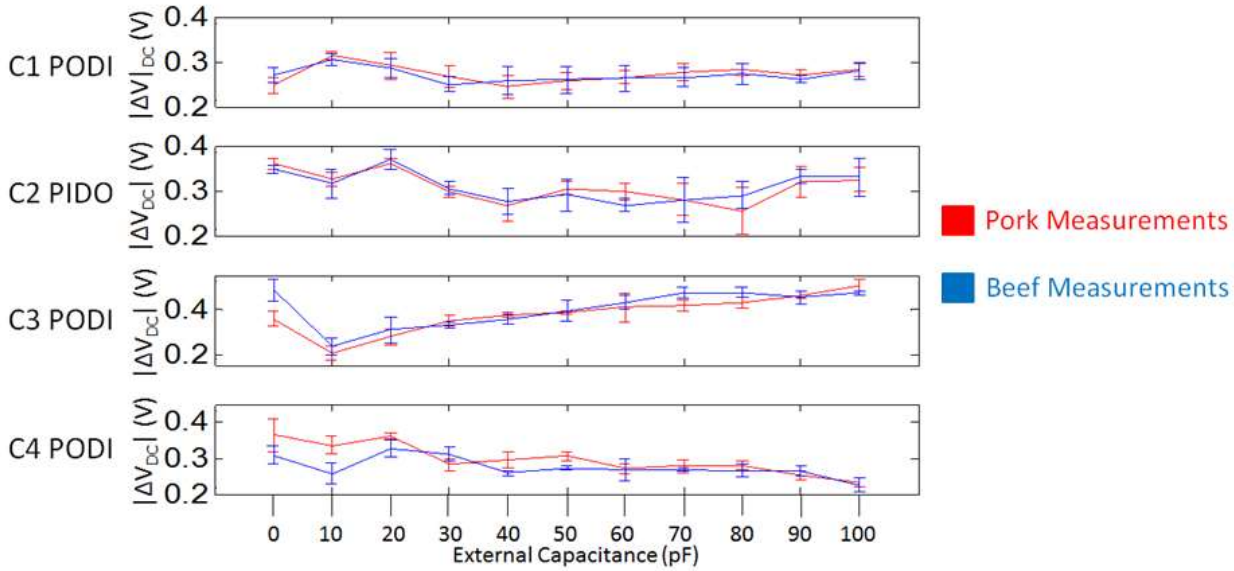

Figure 22: Addition of External Capacitance in the C-Series

Using lock-in amplification on probes C1, C2, and C4 in their optimum lead wire orientation, the voltage difference between no tissue specimen and a tissue specimen stays within the range of 0.2V to 0.4V regardless of external capacitance. Furthermore

the contrast between the two tissue specimens for each of these probes is even smaller. Without external capacitance, C3 in the PODI orientation offered the best contrast of 0.14V between pork and beef tissue samples. With the addition of external capacitance, however, this contrast becomes smaller and the signal of detecting tissue varied from 0.2V to 0.5V. With these results, it can be seen that the addition of external capacitance in the detector coil has a minimal effect on both tissue detection as well as contrast between tissue samples.

In order to investigate why external capacitance has minimal effect, C1 is examined in the optimum PODI orientation. The primary coil is attached to the function generator as usual, but the detector coil is attached to the oscilloscope directly without lock-in amplification. The original detector voltage trace without external capacitance when no sample is present is shown in green in Figure 23. The external variable capacitor is then soldered to the detector coil and set to a low setting of 10pF. The new detector voltage trace when no sample is present is shown in blue in Figure 23. Finally, the variable capacitor is set to a high setting of 100pF and the detector trace without a sample is obtained as shown in red in Figure 23.

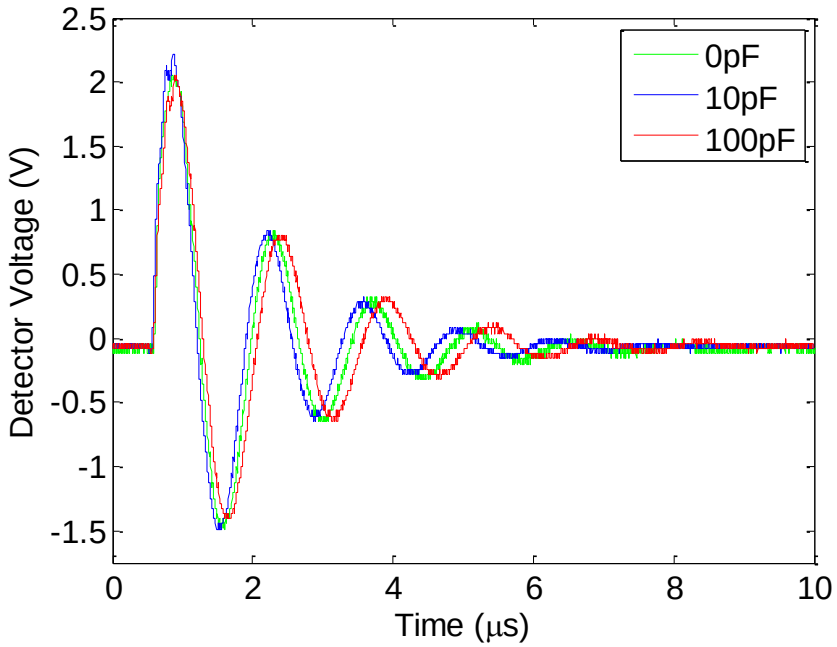

Figure 23: Effect of External Capacitance on Detector Voltage

By examining the effect of external capacitance in Figure 23, it can be seen that simply soldering the variable capacitor to the detector coil affects capacitance. From green to blue in Figure 23, the addition of the external variable capacitor decreases ringing and shifts the peaks left. As explained in Section 4.2, however, the addition of capacitance in the detector coil elongates ringing. When the variable capacitor set to 10pF is added, a change in the capacitance of the solder in the circuit is the only explanation for a decrease in detector voltage ringing. When the variable capacitor is then increased to 100pF, the detector voltage then elongates as expected. At this maximum external capacitance however, the ringing in the detector voltage only lasts approximately 7.5μs and does not last the entire duty cycle of the 99kHz input function which is slightly over 10μs.

Chapter 5: Summary and Conclusions

5.1 Removing a Detector Coil Layer

The most significant difference between B1 and the C-Series is the number of detector coil layers. B1 contains 5 layers and the C-Series contains 4 layers in the detector coil. Because of this decrease in detector coil layers, the inductance of the detector coil drastically decreases from 330µH in B1 to an average of 116µH in the C-Series. The effect that this decrease in inductance has is seen when comparing the detector voltage traces of B1 and the C-Series. Figure 24 shows how the ringing in the detector voltage for B1 lasts significantly longer than that in the C-Series.

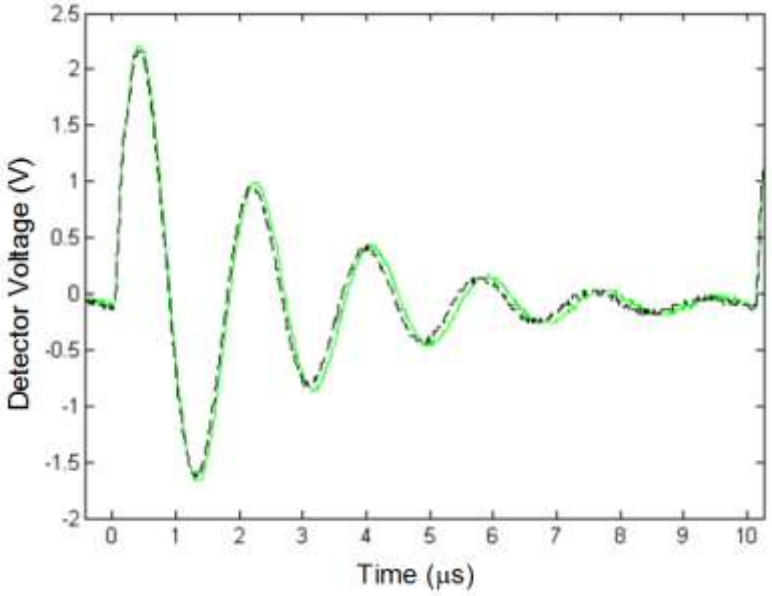

Figure 24: Detector Voltage Ringing in B1

In B1, the ringing lasts the whole duty cycle of the input function and even has a visible peak intersecting with the first peak of the next duty cycle. Removing a single layer of the detector coil significantly decreased the elongation of ringing in the detector coil voltage.

5.2 Wire Insulation Thickness

The insulation of the wire used to wind the probe also affects the design of the EC probe. This is evident when comparing probes C1 and C4 to probes C2 and C3 which have 2.5 times thinner wire insulation. The inferred capacitance of C2 and C3 are higher than those of C1 and C4 for each of the four lead wire orientations. This is expected, however, when considering Equation 7 for parallel plate capacitance. Bringing the conducting cores of the wires closer together with thinner insulation thickness should increase capacitance. This increase in capacitance elongates the ringing in the detector coil. This can be seen by comparing C3 and C4 in the PODI orientation. When in this orientation, the ringing in C3, shown in the upper right quadrant of Figure 20, lasts significantly longer than that of C4, shown in the upper right quadrant of Figure 21. As wire insulation thickness decreases, inferred capacitance increases and detector voltage ringing is elongated.

5.3 Orientation of Lead Wires

The manner in which the EC probe is connected to the function generator and oscilloscope or lock-in amplifier is another factor that affects inferred capacitance and ringing in the detector voltage. Figure 18 through 21 show that different lead wire orientations result in different inferred capacitance and amounts of ringing. For probes C1, C3, and C4, maximum inferred capacitance and maximum ringing were found for the PODI orientation. Furthermore, this lead wire orientation also resulted in maximum contrast between animal tissue samples. For the C-Series of EC probes, the orientation

with the highest inferred capacitance rings the most in the detector voltage and is able to differentiate between animal tissues best.

5.4 External Capacitive Effects

The addition of external capacitance to the detector coil is another manner in which the ringing features can be elongated. Figure 23 shows that as external capacitance is increased from 10pF to 100pF, the peaks in the detector voltage trace shift to the right. This added capacitance in the external circuit does not increase signal or contrast in the C-Series of probes, however. As seen in Figure 22, varying capacitance from 10pF to 100pF does not markedly improve any of the probes ability to detect tissue or differentiate between different types of tissue.

Addition of external capacitance to the C-series of probes did not improve their sensitivity. This result can be explained by comparing Figure 23 with Figure 24. In Figure 23, the ringing of C1 never exceeds approximately 7.5μs while in Figure 24 the ringing of B1 not only lasts the full duty cycle of the input function (slightly over 10μs), but it also runs into and affects the first peak of the next duty cycle. Current studies with B1 have shown that external capacitance does affect the ability of B1 to detect different tissues. Because the ringing in the C-Series is not as elongated as that in B1, however, the effect of external capacitance on the probes in the C-Series is not as significant.

5.5 Comparison of Tissue Measurements with B1 and C-Series

When comparing B1 and the C-Series in ability to detect and differentiate between different types of tissue, B1 is significantly better. Comparing Figure 3 and Figure 22 shows that B1 not only is capable of producing larger voltages from the lock-in amplifier, but is also more capable of discerning between different tissue samples. Figure 3 shows that when a tissue specimen is introduced to B1, the voltage from the lock-in amplifier changes by a maximum of approximately 9.5V. Figure 22, on the other hand,

shows that the the C-Series voltage changes by a maximum of approximately 0.5V when C3 is connected in the PODI orientation. Figure 3 also shows that B1 is capable of discerning dissimilar tissue samples by a maximum of approximately 3.5V. Figure 22, alternatively, shows that the C-Series is is only capable of discerning dissimilar tissue samples by a maximum of approximately 0.15V. In general, B1 offers better signal near tissue as well as better contrast between different tissue specimens. An explanation for this is the significant change in detector voltage signal when a layer is removed as discussed in Section 5.1.

Chapter 6: Recommendations for Future Work

6.1 Inferring Coil Capacitances

In this study, the capacitances of the C-Series of EC probes are inferred by comparing simulated and experimental voltages in the primary and detector coil when a 7 Vpp, 99 kHz sawtooth function is input to the primary coil. When the capacitance is adjusted to match predictions from the circuit element model and experimental results, there is no starting point for the inferred capacitance. A possible way of obtaining this initial inferred capacitance is by examining the two coils of the probe individually. One could apply a 1 kHz sine wave to the primary coil, record the experimental voltage response through an oscilloscope, and repeat for the detector coil. Then the model would be able to infer capacitance for each coil in the probe independently. Moreover, because the inductances of the coils are measured with an LCR meter at 1 kHz, the measured inductances would be closer to the actual experimental inductances. In this work, measured inductances are obtained at 1 kHz, but are implemented in simulated results at 99 kHz. Because the inductance can be frequency dependent, it would be better to use the measured inductance values at the same frequency of 1 kHz when comparing simulations and experimental results. This suggested method of inferring coil capacitances would offer an initial inferred capacitance for both coils rather than finding the two coils' capacitances to be the same as is found in this study. Furthermore, by inferring coil capacitance in this manner, the frequency dependence of capacitance in the probe could be examined.

6.2 Adding Detector Coil Layers

As explained in Section 5.1, the main difference between B1 and the C-Series of EC probes is the removal of a detector coil layer. B1 has 5 detector coil layers and the C-Series has 4 detector coil layers. One layer is removed in the design of the C-Series to allow all lead wires from the probe to be on one side. The removal of this layer, however, significantly decreased the inductance of the detector coil from 330μH in B1 to an average of 116μH in the C-Series. This drastic decrease in inductance shortened the ringing in the detector coil and stopped the last peak from interacting with the first peak in the next duty cycle of the input function. It is suggested to add more layers to the EC probe design to elongate the ringing in the detector coil voltage. An even number of detector coil layers of 6 would allow this ringing to affect the next duty cycle while still maintaining the ability to have all lead wires on the same side of the probe. This increased number of detector coil layers would increase the inductance of the detector and elongate ringing. This could possibly detect more signal between no sample and tissue as well as better differentiate between tissue specimens.

Bibliography

[1] "SEER Stat Fact Sheets: All Cancer Sites." *National Cancer Institute*. Surveillance Epidemiology and End Results. Web. 16 Nov 2013. <http://seer.cancer.gov/statfacts/html/all.html>.

[2] Povoski, Stephen. "Antigen-Directed Cancer Surgery for Primary Colorectal Cancer: 15-Year Survival Analysis." *Surgical Oncology*. (2012): n. page. Print.

[3] Frangioni, John. "The Problem is Background, not Signal."*Molecular Imaging*. 8.6 (2009): 303-304. Print.

[4] De Grand, Alec & Frangioni, John. "An Operational Near-Infrared Fluorescence Imaging System Prototype for Large Animal Surgery." *Technology in Cancer Research & Treatment*. 2.6 (2003): n. page. Print.

[5] Halter, Ryan. "Electrical Impedance Spectroscopy of the Human Prostate." *IEEE Transactions on Biomedical Engineering*. 54.7 (2007): n. page. Print.

[6] Weinberg, Robert. *The Biology of Cancer*, Garland Science, Taylor & Francis, New York, 2007.

[7] Lin, Eugene & Alavi, Abass. (2005). *PET and PET/CT.* New York: Thieme Medical Publishers, Inc.

[8] Wilson, Michelle. *Design and Fabrication of an Electromagnetic Probe for Biomedical Applications*, M.S. Thesis, The Ohio State University, 2011.

[9] Sequin, Emily. *Imaging of Cancer in Tissues Using an Electromagnetic Probe*, M.S. Thesis, The Ohio State University, 2009.

[10] McFerran, Jennifer. *An Electromagnetic Method for Cancer Detection*, PhD Dissertation. The Ohio State University, 2009.

[11] Stanford Research Systems. (1989). *Model SR510 Lock-In Amplifier.* Sunnyvale, CA: Stanford Research Systems.

Appendix A: MATLAB Inductance Calculator

```
% ALL MUTUAL AND SELF INDUCTANCES, Resistances of Wire Loops

% Program calculates the self inductances of the driver coil, receiver
% coil and all loops, the mutual inductances between all elements
% (driver-receiver, receiver-driver, driver-loop, loop-driver,
% loop-receiver, receiver-loop)
% Program also calculates the internal resistance and inductance of a
loop of round wire
% as the real and imaginary parts (respectively) of the wire's total
% impedance.  Total impedance calculated using exact solution given in
% Ramo, "Fields & Waves in Communication Electronics," 1984.

% Inputs:
%         [L] Length of probe, m
%         [dd] diameter of wire used to construct probe,m
%         [d1p] inner diameter primary coil, m
%         [d2p] outer diameter primary coil, m
%         [D1d] inner diameter detector coil, m
%         [D2d] outer diameter detector coil, m
%         [M] number of turns in r-direction (layers), primary coil
%         [P] number of turns in r-direction (layers), detector coil
%         [Nd] number of turns/layer, detector coil
%         [Np] number of turns/layer, primary coil

% Outputs:
%         [Lp] Self inductance Primary coil, H
%         [Ld] Self inductance Detector coil, H
%         [Mpd] Mutual inductance from driver(primary) to receiver
%               (detector), H
%         [Mdp] Mutual inductance from the receiver to driver, H

function [Lp Ld  Mpd Mdp ]= Inductances_Calculator(L, dd, d1p, d2p,
D1d,D2d, M, P, Np, Nd)

rr=dd/2;
d1=d1p+dd; %m, inner diameter of driver coil
a1=d1/2; %m, inner radius of driver coil
d2=d2p-dd; %m, outer diameter of driver coil
a2=d2/2; %m, outer radius of driver coil
D2=D1d+dd; %m, inner diameter of receiver coil
R2=D2/2; %inner radius of receiver coil
D3=D2d-dd; %m, outer diameter of receiver coil
```

```
R3=D3/2; %m, outer radius of receiver coil

% EM properties
mu0=4*pi*10^(-7); %V*sec/A/m, magnetic permittivity of vacuum
I=1;%A, current (NB: all inductance values independent of current,
since it
    %divides out at the end

% SELF INDUCTANCES-------------------------------------------------------
---
% 1. Driver coil
Z=linspace(0,L,Np);
a=linspace(a1,a2,M);

clear flux_single_turn flux A k2 K E
for e=1:M %r-direction, driver coil
    for f=1:Np %z-direction, driver coil
        for i=1:M %r-direction, driver coil
            for j=1:Np %z-direction, driver coil
                k2=4*a(i)*(a(e)-rr)*((a(i)+a(e)-rr)^2+(Z(f)-Z(j))^2)^(-
1);
                [K,E] = ellipke(k2);
                A=mu0*I/pi/sqrt(k2)*sqrt(a(i)/(a(e)-rr))*((1-.5*k2)*K-
E);
                flux_single_turn(i,j)=2*pi*(a(e)-rr)*A;
            end
        end
        flux(e,f)=sum(sum(flux_single_turn));
    end
end
Lp=sum(sum(flux))/I %calculated self inductance of driver

%2. Receiver coil
R=linspace(R2,R3,P); %receiver coil
ZZ=linspace(0,L,Nd); %receiver coil

clear flux_single_turn flux A k2 K E
for e=1:P %r-direction, receiver coil
    for f=1:Nd %z-direction, receiver coil
        for i=1:P %r-direction, receiver coil
            for j=1:Nd %z-direction, receiver coil
                k2=4*R(i)*(R(e)-rr)*((R(i)+(R(e)-rr))^2+(ZZ(f)-
ZZ(j))^2)^(-1);
                [K,E] = ellipke(k2);
                A=mu0*I/pi/sqrt(k2)*sqrt(R(i)/(R(e)-rr))*((1-.5*k2)*K-
E);
                flux_single_turn(i,j)=2*pi*(R(e)-rr)*A;
            end
        end
        flux(e,f)=sum(sum(flux_single_turn));
    end
end

Ld=sum(sum(flux))/I %calculated self inductance of receiver
```

```
% MUTUAL INDUCTANCES-----------------------------------------------------
---
%1. Driver to receiver
clear flux_single_turn flux A k2 K E
for e=1:P %r-direction, receiver coil
    for f=1:Nd %z-direction, receiver coil
        for i=1:M %r-direction, driver coil
            for j=1:Np %z-direction, driver coil
                k2=4*a(i)*R(e)*((a(i)+R(e))^2+(ZZ(f)-Z(j))^2)^(-1);
                [K,E] = ellipke(k2);
                A=mu0*I/pi/sqrt(k2)*sqrt(a(i)/R(e))*((1-.5*k2)*K-E);
                flux_single_turn(i,j)=2*pi*R(e)*A;
            end
        end
        flux(e,f)=sum(sum(flux_single_turn));
    end
end

Mpd=sum(sum(flux))/I

%2. Receiver to driver
clear flux_single_turn flux A k2 K E
for i=1:M %r-direction, driver coil
    for j=1:Np %z-direction, driver coil
        for e=1:P %r-direction, receiver coil
            for f=1:Nd %z-direction, receiver coil
                k2=4*R(e)*a(i)*((R(e)+a(i))^2+(Z(j)-ZZ(f))^2)^(-1);
                [K,E] = ellipke(k2);
                A=mu0*I/pi/sqrt(k2)*sqrt(R(e)/a(i))*((1-.5*k2)*K-E);
                flux_single_turn(e,f)=2*pi*a(i)*A;
            end
        end
        flux(i,j)=sum(sum(flux_single_turn));
    end
end
Mdp=sum(sum(flux))/I
```

Appendix B: MATLAB Code used to Infer Capacitance

Runner Function

This function is used to open the graphical interface.

```
function Detector_Runner_Comparison_One_Plot
clear all; close all; clc;

%setup main figure
mainfig = figure(1);
set(mainfig,'Position',[10 60 1900 930]);
set(mainfig,'tag','mainfig');
set(mainfig,'Toolbar','figure')

%set font sizes
ud.design.Heading = 40; %40 for Scott Lab 40 for laptop
ud.design.Label   = 20; %20 for Scott Lab 15 for laptop
ud.design.Text    = 15; %15 for Scott Lab 10 for laptop
ud.design.Box     = 12; %12 for Scott Lab 10 for laptop

subplot(1,1,1)
set(subplot(1,1,1),'OuterPosition',[0.1 0.02 0.9 0.9]);
xlabel('Time (s)','FontSize',ud.design.Label)
ylabel('Voltage (V)','FontSize',ud.design.Label)
set(gca,'fontsize',ud.design.Label)
title('Experimental and Simulated Voltages v
Time','FontSize',ud.design.Label)
grid on

%Initialize design parameters with C1 constants (capacitance guesses)
ud.design.Points= 10000;          %data points per period
ud.design.Wav   = 1;             %sawtooth
ud.design.Amp   = 7;             %volts
ud.design.Freq  = 99;            %kHz
ud.design.Rb    = 578.2;         %ohms
ud.design.Cp    = 300*10^-12;    %farads
ud.design.Rp    = 1.68;          %ohms
ud.design.Lp    = 26.4*10^-6;    %henries
ud.design.Cd    = 300*10^-12;    %farads
ud.design.Rd    = 2.92;          %ohms
ud.design.Ld    = 111.9*10^-6;   %henries
ud.design.Mpd   = 46.879*10^-6;  %henries
ud.design.Probe = 1;             %C1
```

```
ud.design.HO    = 1;              %PI DI
ud.design.Sign  = 1;              %positive
ud.design.Data=xlsread('scope_01_pidi.xlsx','A3:E20002'); %1st data set
TimeStep=1/(ud.design.Freq*1000)/ud.design.Points;
LastTime=6/(ud.design.Freq*1000);
ud.design.InputTime=(0:TimeStep:LastTime);
Max=ud.design.Amp/2;
FreqTime=2*pi*ud.design.Freq*1000*ud.design.InputTime;
ud.design.InputVoltage=Max*sawtooth(FreqTime,1);

%%%%%%%%%%%%%%%%%%%%%%%%%%%%
%%%%% UIcontrols below %%%%%
%%%%%%%%%%%%%%%%%%%%%%%%%%%%

%left bound for text
xtext = .035;
%upper bound for text
ytext = .8;
%width of textbox
wtext = .075;
%height of textbox
htext = .02;
%vertical spacing
ytextspace = .03;
%left bound for edits
xedit = xtext + .08;
%width of edits
wedit = .05;

%Headings
ud.obj.Title = uicontrol('Style','text','string',...
    'Eddy Current Probe Model','Units','normalized',...
    'Position',[.25 .9 .5 .05],'BackgroundColor',[0.8 0.8 0.8],...
    'FontSize',ud.design.Heading,'FontName','Stencil');
ud.obj.uiBanner = uicontrol('Style','text','string',...
    'Design Parameters','Units','normalized','Position',...
    [xtext-.01 ytext+ytextspace wtext+.075 htext+.01],'FontSize',...
    ud.design.Label,'BackgroundColor',[0.8 0.8 0.8]);

%Waveform
ud.obj.uiWav = uicontrol('Style', 'popup','Units','normalized',...
    'String','Sawtooth|Square|Sine|O-Scope','Position',...
    [xedit ytext wedit htext],'FontSize',ud.design.Box,'Callback',
@setWav);
ud.obj.uiWavtxt = uicontrol('Style','text','string','Waveform',...
    'HorizontalAlignment','left','Units','normalized',...
    'Position',[xtext ytext wtext htext],'FontSize',ud.design.Text,...
    'BackgroundColor',[0.8 0.8 0.8]);

%Amplitude
ud.obj.uiAmp = uicontrol('Style','edit','string',ud.design.Amp,...
    'Units','normalized','Position',...
    [xedit ytext-ytextspace wedit htext],'FontSize',ud.design.Box,...
```

```
    'Callback', @setAmp);
ud.obj.uiAmptxt = uicontrol('Style','text','Units','normalized',...
    'HorizontalAlignment','left','string','P2P Amplitude (Volts)',...
    'Position',[xtext ytext-ytextspace wtext
htext],'FontSize',ud.design.Text,...
    'BackgroundColor',[0.8 0.8 0.8]);

%Frequency
ud.obj.uiFreq = uicontrol('Style','edit','string',ud.design.Freq,...
    'Units','normalized','Position',...
    [xedit ytext-2*ytextspace wedit htext],'FontSize',ud.design.Box,...
    'Callback', @setFreq);
ud.obj.uiFreqtxt = uicontrol('Style','text','Units','normalized',...
    'HorizontalAlignment','left','string','Frequency (kHz)',...
    'Position',[xtext ytext-2*ytextspace wtext
htext],'FontSize',ud.design.Text,...
    'BackgroundColor',[0.8 0.8 0.8]);

%Back Resistance
ud.obj.uiRb = uicontrol('Style','edit','string',ud.design.Rb,...
    'Units','normalized','Position',...
    [xedit ytext-4*ytextspace wedit htext],'FontSize',ud.design.Box,...
    'Callback', @setRb);
ud.obj.uiRbtxt = uicontrol('Style','text','Units','normalized',...
    'HorizontalAlignment','left','string','Rb (Ohms)',...
    'Position',[xtext ytext-4*ytextspace wtext
htext],'FontSize',ud.design.Text,...
    'BackgroundColor',[0.8 0.8 0.8]);

%Primary Capacitance
ud.obj.uiCp = uicontrol('Style','edit','string',ud.design.Cp,...
    'Units','normalized','Position',...
    [xedit ytext-6*ytextspace wedit htext],'FontSize',ud.design.Box,...
    'Callback', @setCp);
ud.obj.uiCptxt = uicontrol('Style','text','Units','normalized',...
    'HorizontalAlignment','left','string','Cp (Farads)',...
    'Position',[xtext ytext-6*ytextspace wtext
htext],'FontSize',ud.design.Text,...
    'BackgroundColor',[0.8 0.8 0.8]);

%Primary Resistance
ud.obj.uiRp = uicontrol('Style','edit','string',ud.design.Rp,...
    'Units','normalized','Position',...
    [xedit ytext-7*ytextspace wedit htext],'FontSize',ud.design.Box,...
    'Callback', @setRp);
ud.obj.uiRptxt = uicontrol('Style','text','Units','normalized',...
    'HorizontalAlignment','left','string','Rp (Ohms)',...
    'Position',[xtext ytext-7*ytextspace wtext
htext],'FontSize',ud.design.Text,...
    'BackgroundColor',[0.8 0.8 0.8]);

%Primary Inductance
ud.obj.uiLp = uicontrol('Style','edit','string',ud.design.Lp,...
    'Units','normalized','Position',...
    [xedit ytext-8*ytextspace wedit htext],'FontSize',ud.design.Box,...
```

```
    'Callback', @setLp);
ud.obj.uiLptxt = uicontrol('Style','text','Units','normalized',...
    'HorizontalAlignment','left','string','Lp (Henries)',...
    'Position',[xtext ytext-8*ytextspace wtext
htext],'FontSize',ud.design.Text,...
    'BackgroundColor',[0.8 0.8 0.8]);

%Detector Capacitance
ud.obj.uiCd = uicontrol('Style','edit','string',ud.design.Cd,...
    'Units','normalized','Position',...
    [xedit ytext-10*ytextspace wedit
htext],'FontSize',ud.design.Box,...
    'Callback', @setCd);
ud.obj.uiCdtxt = uicontrol('Style','text','Units','normalized',...
    'HorizontalAlignment','left','string','Cd (Farads)',...
    'Position',[xtext ytext-10*ytextspace wtext
htext],'FontSize',ud.design.Text,...
    'BackgroundColor',[0.8 0.8 0.8]);

%Detector Resistance
ud.obj.uiRd = uicontrol('Style','edit','string',ud.design.Rd,...
    'Units','normalized','Position',...
    [xedit ytext-11*ytextspace wedit
htext],'FontSize',ud.design.Box,...
    'Callback', @setRd);
ud.obj.uiRptxt = uicontrol('Style','text','Units','normalized',...
    'HorizontalAlignment','left','string','Rd (Ohms)',...
    'Position',[xtext ytext-11*ytextspace wtext
htext],'FontSize',ud.design.Text,...
    'BackgroundColor',[0.8 0.8 0.8]);

%Detector Inductance
ud.obj.uiLd = uicontrol('Style','edit','string',ud.design.Ld,...
    'Units','normalized','Position',...
    [xedit ytext-12*ytextspace wedit
htext],'FontSize',ud.design.Box,...
    'Callback', @setLd);
ud.obj.uiLdtxt = uicontrol('Style','text','Units','normalized',...
    'HorizontalAlignment','left','string','Ld (Henries)',...
    'Position',[xtext ytext-12*ytextspace wtext
htext],'FontSize',ud.design.Text,...
    'BackgroundColor',[0.8 0.8 0.8]);

%Mutual Inductance
ud.obj.uiMpd = uicontrol('Style','edit','string',ud.design.Mpd,...
    'Units','normalized','Position',...
    [xedit ytext-14*ytextspace wedit
htext],'FontSize',ud.design.Box,...
    'Callback', @setMpd);
ud.obj.uiMpdtxt = uicontrol('Style','text','Units','normalized',...
    'HorizontalAlignment','left','string','Mpd (Henries)',...
    'Position',[xtext ytext-14*ytextspace wtext
htext],'FontSize',ud.design.Text,...
    'BackgroundColor',[0.8 0.8 0.8]);
```

```
%Experimental Probe
ud.obj.uiProbe = uicontrol('Style', 'popup','Units','normalized',...
    'String','C1|C2|C3|C4','Position',...
    [xedit ytext-16*ytextspace wedit
htext],'FontSize',ud.design.Box,...
    'Callback', @setProbe);
ud.obj.uiProbetxt = uicontrol('Style','text','string','Probe',...
    'HorizontalAlignment','left','Units','normalized',...
    'Position',[xtext ytext-16*ytextspace wtext
htext],'FontSize',ud.design.Text,...
    'BackgroundColor',[0.8 0.8 0.8]);

%Experimental Hookup Orientation
ud.obj.uiHO = uicontrol('Style', 'popup','Units','normalized',...
    'String','PI DI|PO DI|PI DO|PO DO','Position',...
    [xedit ytext-17*ytextspace wedit
htext],'FontSize',ud.design.Box,...
    'Callback', @setHO);
ud.obj.uiHOtxt = uicontrol('Style','text','string','Hookup
Orientation',...
    'HorizontalAlignment','left','Units','normalized',...
    'Position',[xtext ytext-17*ytextspace wtext
htext],'FontSize',ud.design.Text,...
    'BackgroundColor',[0.8 0.8 0.8]);

%Sign of Detector Trace
ud.obj.uiSign = uicontrol('Style', 'popup','Units','normalized',...
    'String','Positive|Negative','Position',...
    [xedit ytext-18*ytextspace wedit
htext],'FontSize',ud.design.Box,...
    'Callback', @setSign);
ud.obj.uiSigntxt = uicontrol('Style','text','string','Detector
Trace',...
    'HorizontalAlignment','left','Units','normalized',...
    'Position',[xtext ytext-18*ytextspace wtext
htext],'FontSize',ud.design.Text,...
    'BackgroundColor',[0.8 0.8 0.8]);

%Save to Excel Button
ud.obj.uiExcel_Button=uicontrol('Style','pushbutton','string',...
    'Export to Excel','Units','normalized','Position',...
    [xtext ytext-20*ytextspace wtext htext*2],...
    'FontSize',ud.design.Text,'Callback', @excel_button);

set(mainfig,'userdata',ud)
DetectEval_Comparison_One_Plot(ud)
end

%%%%%%%%%%%%%%%%%%%%%%%%%%%%%%%%%%%%%%%%%%%%%%%%%%%%%%%%%%%%%%%%%%%
%%%%% Subfunctions to change the design parameters %%%%%
%%%%%%%%%%%%%%%%%%%%%%%%%%%%%%%%%%%%%%%%%%%%%%%%%%%%%%%%%%%%%%%%%%%

function setWav(hObj,event)
    user_input = get(hObj,'Value');
```

```
    ud = get(findobj('tag','mainfig'),'userdata');
    ud.design.Wav = user_input;
    [Vo,tspan] =
createWav(ud.design.Data,ud.design.Freq,ud.design.Points,ud.design.Wav,
ud.design.Amp);
    %put waveform into structure
    ud.design.InputVoltage = Vo;
    ud.design.InputTime = tspan;
    set(findobj('tag','mainfig'),'userdata',ud)
    DetectEval_Comparison_One_Plot(ud)
end

function setAmp (hObject, eventdata, handles)
    user_input = str2double(get(hObject,'string'));
    if isnan(user_input)
      errordlg('You must enter a numeric value','Bad Input','modal')
      uicontrol(hObject)
      return
    end
    ud = get(findobj('tag','mainfig'),'userdata');
    ud.design.Amp = user_input;
    [Vo,tspan] =
createWav(ud.design.Data,ud.design.Freq,ud.design.Points,ud.design.Wav,
ud.design.Amp);
    %put waveform into structure
    ud.design.InputVoltage = Vo;
    ud.design.InputTime = tspan;
    set(findobj('tag','mainfig'),'userdata',ud)
    DetectEval_Comparison_One_Plot(ud)
end

function setFreq (hObject, eventdata, handles)
    user_input = str2double(get(hObject,'string'));
    if isnan(user_input)
      errordlg('You must enter a numeric value','Bad Input','modal')
      uicontrol(hObject)
      return
    end
    ud = get(findobj('tag','mainfig'),'userdata');
    ud.design.Freq = user_input;
    [Vo,tspan] =
createWav(ud.design.Data,ud.design.Freq,ud.design.Points,ud.design.Wav,
ud.design.Amp);
    %put waveform into structure
    ud.design.InputVoltage = Vo;
    ud.design.InputTime = tspan;
    set(findobj('tag','mainfig'),'userdata',ud)
    DetectEval_Comparison_One_Plot(ud)
end

function setRb (hObject, eventdata, handles)
    user_input = str2double(get(hObject,'string'));
    if isnan(user_input)
      errordlg('You must enter a numeric value','Bad Input','modal')
      uicontrol(hObject)
```

```
      return
    end
    ud = get(findobj('tag','mainfig'),'userdata');
    ud.design.Rb = user_input;
    set(findobj('tag','mainfig'),'userdata',ud)
    DetectEval_Comparison_One_Plot(ud)
end

function setCp (hObject, eventdata, handles)
    user_input = str2double(get(hObject,'string'));
    if isnan(user_input)
      errordlg('You must enter a numeric value','Bad Input','modal')
      uicontrol(hObject)
      return
    end
    ud = get(findobj('tag','mainfig'),'userdata');
    ud.design.Cp = user_input;
    set(findobj('tag','mainfig'),'userdata',ud)
    DetectEval_Comparison_One_Plot(ud)
end

function setRp (hObject, eventdata, handles)
    user_input = str2double(get(hObject,'string'));
    if isnan(user_input)
      errordlg('You must enter a numeric value','Bad Input','modal')
      uicontrol(hObject)
      return
    end
    ud = get(findobj('tag','mainfig'),'userdata');
    ud.design.Rp = user_input;
    set(findobj('tag','mainfig'),'userdata',ud)
    DetectEval_Comparison_One_Plot(ud)
end

function setLp (hObject, eventdata, handles)
    user_input = str2double(get(hObject,'string'));
    if isnan(user_input)
      errordlg('You must enter a numeric value','Bad Input','modal')
      uicontrol(hObject)
      return
    end
    ud = get(findobj('tag','mainfig'),'userdata');
    ud.design.Lp = user_input;
    set(findobj('tag','mainfig'),'userdata',ud)
    DetectEval_Comparison_One_Plot(ud)
end

function setCd (hObject, eventdata, handles)
    user_input = str2double(get(hObject,'string'));
    if isnan(user_input)
      errordlg('You must enter a numeric value','Bad Input','modal')
      uicontrol(hObject)
      return
    end
    ud = get(findobj('tag','mainfig'),'userdata');
```

```
    ud.design.Cd = user_input;
    set(findobj('tag','mainfig'),'userdata',ud)
    DetectEval_Comparison_One_Plot(ud)
end

function setRd (hObject, eventdata, handles)
    user_input = str2double(get(hObject,'string'));
    if isnan(user_input)
      errordlg('You must enter a numeric value','Bad Input','modal')
      uicontrol(hObject)
      return
    end
    ud = get(findobj('tag','mainfig'),'userdata');
    ud.design.Rd = user_input;
    set(findobj('tag','mainfig'),'userdata',ud)
    DetectEval_Comparison_One_Plot(ud)
end

function setLd (hObject, eventdata, handles)
    user_input = str2double(get(hObject,'string'));
    if isnan(user_input)
      errordlg('You must enter a numeric value','Bad Input','modal')
      uicontrol(hObject)
      return
    end
    ud = get(findobj('tag','mainfig'),'userdata');
    ud.design.Ld = user_input;
    set(findobj('tag','mainfig'),'userdata',ud)
    DetectEval_Comparison_One_Plot(ud)
end

function setMpd (hObject, eventdata, handles)
    user_input = str2double(get(hObject,'string'));
    if isnan(user_input)
      errordlg('You must enter a numeric value','Bad Input','modal')
      uicontrol(hObject)
      return
    end
    ud = get(findobj('tag','mainfig'),'userdata');
    ud.design.Mpd = user_input;
    set(findobj('tag','mainfig'),'userdata',ud)
    DetectEval_Comparison_One_Plot(ud)
end

function setProbe(hObj,event)
    user_input = get(hObj,'Value');
    ud = get(findobj('tag','mainfig'),'userdata');
    ud.design.Probe = user_input;
    ud.design.Data = readData(ud.design.Probe,ud.design.HO);
    set(findobj('tag','mainfig'),'userdata',ud)
    DetectEval_Comparison_One_Plot(ud)
end

function setHO(hObj,event)
    user_input = get(hObj,'Value');
```

```
    ud = get(findobj('tag','mainfig'),'userdata');
    ud.design.HO = user_input;
    ud.design.Data = readData(ud.design.Probe,ud.design.HO);
    set(findobj('tag','mainfig'),'userdata',ud)
    DetectEval_Comparison_One_Plot(ud)
end

function setSign(hObj,event)
    user_input = get(hObj,'Value');
    ud = get(findobj('tag','mainfig'),'userdata');
    ud.design.Sign = user_input;
    set(findobj('tag','mainfig'),'userdata',ud)
    DetectEval_Comparison_One_Plot(ud)
end

function excel_button(hObject, eventdata, handles)
    ud = get(findobj('tag','mainfig'),'userdata');
    export(1,1:3)=[ud.design.Wav,ud.design.Amp,ud.design.Freq];
    export(1,4:6)=[ud.design.Rb,ud.design.Cp,ud.design.Rp];
    export(1,7:9)=[ud.design.Lp,ud.design.Cd,ud.design.Rd];
    export(1,10:12)=[ud.design.Ld,ud.design.Mpd,ud.design.Probe];
    export(1,13:14)=[ud.design.HO,ud.design.Sign];
    filename = 'Design_Points.xlsx';
    excel=xlsread(filename,1,'B2:M20');
    [R,C]=size(excel);
    if R==0
        excel(1,1:14)=export;
        xlswrite(filename,excel,1,'B2:O2');
    end
    if R~=0
        excel(R+1,1:14)=export;
        xlswrite(filename,excel,1,'B2:O21');
    end
end

function[Vo,tspan] = createWav(Data,Freq,Points,Wav,Amp)
    %separate Data into time and input
    time=Data(:,1);
    input=Data(:,3);
    %create input waveform
    tspan=(0:1/Freq/1000/Points:6/Freq/1000);
    w=2*pi*Freq*1000;
    if Wav==1
        %sawtooth wave
        Vo=Amp/2*sawtooth(w*tspan,1);
    elseif Wav==2
     %square wave
        Vo=Amp/2*square(w*tspan);
    elseif Wav==3
        %sin wave
        Vo=Amp/2*sin(w*tspan);
    elseif Wav==4
        i=1;
        done=0;
        while done<2
```

```
            if done==1 && input(i)<0 && input(i-1)>=0
               address2=i-1;
               done=done+1;
            end
            if done==0 && input(i)<0 && input(i-1)>=0
               address1=i-1;
               done=done+1;
               %move over 3/4 of period to avoid noise at zero crossing
               tinterval=time(i)-time(i-1);
               period=1/Freq/1000;
               moveover=ceil(3/4*period/tinterval);
               i=i+moveover;
            end
        i=i+1;
        end
    expVo=input(address1:address2);
    exptime=time(address1:address2);
    exptime1=exptime-exptime(1);
    Vo=[expVo;expVo;expVo;expVo;expVo;expVo];
    tspan=linspace(0,6*exptime1(length(exptime1)),6*length(exptime1));
    end
end

function[Data] = readData(Probe,HO)
if Probe == 1
    if HO == 1
        Data=xlsread('scope_01_pidi.xlsx','A3:E20002');
    end
    if HO == 2
        Data=xlsread('scope_01_podi.xlsx','A3:E20002');
    end
    if HO == 3
        Data=xlsread('scope_01_pido.xlsx','A3:E20002');
    end
    if HO == 4
        Data=xlsread('scope_01_podo.xlsx','A3:E20002');
    end
end
if Probe == 2
    if HO == 1
        Data=xlsread('scope_02_pidi.xlsx','A3:E20002');
    end
    if HO == 2
        Data=xlsread('scope_02_podi.xlsx','A3:E20002');
    end
    if HO == 3
        Data=xlsread('scope_02_pido.xlsx','A3:E20002');
    end
    if HO == 4
        Data=xlsread('scope_02_podo.xlsx','A3:E20002');
    end
end
if Probe == 3
    if HO == 1
        Data=xlsread('scope_03_pidi.xlsx','A3:E20002');
```

```
    end
    if HO == 2
        Data=xlsread('scope_03_podi.xlsx','A3:E20002');
    end
    if HO == 3
        Data=xlsread('scope_03_pido.xlsx','A3:E20002');
    end
    if HO == 4
        Data=xlsread('scope_03_podo.xlsx','A3:E20002');
    end
end
if Probe == 4
    if HO == 1
        Data=xlsread('scope_04_pidi.xlsx','A3:E20002');
    end
    if HO == 2
        Data=xlsread('scope_04_podi.xlsx','A3:E20002');
    end
    if HO == 3
        Data=xlsread('scope_04_pido.xlsx','A3:E20002');
    end
    if HO == 4
        Data=xlsread('scope_04_podo.xlsx','A3:E20002');
    end
end
end
```

Evaluation Function

This function is used to call the solver function and re-plot the results each time a design parameter is changed.

```
function DetectEval_Comparison_One_Plot (struct)

%input simulated input waveform data
Vo=struct.design.InputVoltage;
tspan=struct.design.InputTime;
Sign  = struct.design.Sign;
ud.design.Label= struct.design.Label;
Data = struct.design.Data;
time=Data(:,1);
sync=Data(:,2);
input=Data(:,3);
primary=Data(:,4);
detector=Data(:,5);

%Solve System
initial=[0 0 0 0];
%solve using equation solver DetectFunc
```

```
[T,Y]=ode15s(@DetectFunc,tspan,initial);

%if necessary flip sign of simulated to match experimental
if Sign==2
    Y(:,2)=Y(:,2)*-1;
end

%start experimental data with V=0 step down in sawtooth input
i=1;
done=0;
while done==0
    if input(i)<0
            time1=time(i-1:length(time));
            input1=input(i-1:length(input));
            primary1=primary(i-1:length(primary));
            detector1=detector(i-1:length(detector));
            done=1;
    end
   i=i+1;
end

%shift experimental data to match up with simulated data
time2=time1-time1(1)+3/struct.design.Freq/1000;

%plot experimental and simulated
subplot(1,1,1)
set(subplot(1,1,1),'OuterPosition',[0.1 0.02 0.9 0.9]);
plot(tspan,Vo,'k')
hold on
plot(T,Y(:,1),'b', T,Y(:,2), 'r');
plot(time2,input1,'g',time2,primary1,'c',time2,detector1,'m');
hold off
% axis([3/struct.design.Freq/1000 5/struct.design.Freq/1000 -
struct.design.Amp/2 struct.design.Amp/2])
axis([3/struct.design.Freq/1000 5/struct.design.Freq/1000 -3.5 3.5])
h_legend=legend('Vo Simulated','Vp Simulated','Vd Simulated',...
    'Vo Experimental','Vp Experimental','Vd Experimental');
set(h_legend,'FontSize',ud.design.Label)
xlabel('Time (s)','FontSize',ud.design.Label)
ylabel('Volts (V)','FontSize',ud.design.Label)
set(gca,'fontsize',ud.design.Label)
title('Experimental and Simulated Voltages v
Time','FontSize',ud.design.Label)
grid on
end
```

Solver Function

This function is used to solve the differential equations of the EC probe model for the voltages and currents in the primary and detector coils.

```
function [ dy ] = DetectFunc(t,y)
%DetectFunc solves the four detector model ODEs
%Vp=y(1) Vd=y(2) Ip=y(3) Id=y(4) dy=derivative matrix

%get system data
data = get(findobj('tag','mainfig'),'userdata');

Rb    = data.design.Rb;
Cp    = data.design.Cp;
Rp    = data.design.Rp;
Lp    = data.design.Lp;
Cd    = data.design.Cd;
Rd    = data.design.Rd;
Ld    = data.design.Ld;
Mpd   = data.design.Mpd;
InputVoltage = data.design.InputVoltage;
InputTime    = data.design.InputTime;

%linear interpolate experimental data
Vo=interp1(InputTime,InputVoltage,t);

%solve [a]*[dy]=[b]
a=[Cp 0 0 0;0 Cd 0 0;0 0 Lp Mpd;0 0 Mpd Ld];
b=[(Vo-y(1))./Rb-y(3); y(4);y(1)-Rp.*y(3); -y(2)-Rd.*y(4)];
dy=a\b;
end
```